PERGAMON

Deep-Sea Research II 48 (2001) 1127–1172

DEEP-SEA RESEARCH
PART II

www.elsevier.com/locate/dsr2

Primary productivity and its regulation in the Arabian Sea during 1995

Richard T. Barber[a,*], John Marra[b], Robert C. Bidigare[c], Louis A. Codispoti[d], David Halpern[e], Zackary Johnson[a], Mikel Latasa[f], Ralf Goericke[g], Sharon L. Smith[h]

[a]*Duke University, Nicholas School of the Environment, Beaufort, NC 28516, USA*
[b]*Lamont-Doherty Earth Observatory, Palisades, NY 10964, USA*
[c]*University of Hawaii, Honolulu, HI 96822, USA*
[d]*University of Maryland, Horn Point Laboratory, Cambridge, MD 21613, USA*
[e]*Jet Propulsion Laboratory, California Institute of Technology, Pasadena, CA 91109, USA*
[f]*Instituto de Ciencias del Mar, Barcelona, Spain*
[g]*Scripps Institution of Oceanography, La Jolla, CA 92093-0218, USA*
[h]*University of Miami, Rosenstiel School of Marine and Atmospheric Science, Miami, FL 33149, USA*

Received 23 June 1999; received in revised form 25 May 2000; accepted 7 July 2000

Abstract

The annual cycle of monsoon-driven variability in primary productivity was studied in 1995 during the Arabian Sea Expedition as part of the United States Joint Global Ocean Flux Studies (US JGOFS). This paper describes the seasonal progression of productivity and its regulation on a section which ran from the coast of Oman to about 1000 km offshore in the central Arabian Sea at 65°E. During the SW Monsoon (June–mid-September), the coolest water and highest nutrient concentrations were close to the coast, although they extended offshore to about 800 km; during the January NE Monsoon, deep convective mixing provided nutrients to the mixed layer in the region 400 – 1000 km offshore. As expected, the SW Monsoon was the most productive season (123 ± 9 mmol C m^{-2} d^{-1}) along the southern US JGOFS section from the coast to 1000 km offshore, but productivity in the NE Monsoon was surprisingly high (112 ± 7 mmol C m^{-2} d^{-1}). There was no onshore/offshore gradient in primary productivity from 150 to 1000 km off the Omani coast in 1995, and there was no evidence of light limitation of either primary productivity or photosynthetic performance (P^{B}_{opt}) from deep convective mixing during the NE Monsoon, deep wind mixing during the SW Monsoon or offshore Ekman downwelling during the SW Monsoon. Productivity during the Spring Intermonsoon (86 ± 6 mmol C m^{-2} d^{-1}) was much higher than in oligotrophic regions such as the tropical Pacific Ocean (29 ± 2 mmol C m^{-2} d^{-1}) or the North Pacific gyre region (32 ± 8 mmol C m^{-2} d^{-1}).

* Corresponding author. Fax: + 1-252-504-7648.
E-mail address: rbarber@duke.edu (R.T. Barber).

0967-0645/01/$ - see front matter
PII: S0967-0645(00)00134-X

The 1995 annual mean productivity (111 ± 11 mmol C m^{-2} d^{-1}) along this section from the Omani coast to the central Arabian Sea was about equal to the spring bloom maximum (107 ± 23 mmol C m^{-2} d^{-1}) during the 1989 North Atlantic Bloom Experiment (NABE) and the equatorial, 1°N–1°S wave guide maximum (95 ± 6 mmol C m^{-2} d^{-1}) in the Pacific Ocean during the 1992 EqPac study. The 1995 SW Monsoon primary productivity was similar to the mean value observed in the same region in 1994 by the Arabesque Expedition (127 ± 14 mmol C m^{-2} d^{-1}) and in 1964 by the ANTON BRUUN Expedition (115 ± 27 mmol C m^{-2} d^{-1}). During the 1995 SW Monsoon, strong, narrow and meandering current filaments extended from the region of coastal upwelling to about 700 km offshore; these filaments had levels of biomass, primary productivity, chlorophyll-specific productivity and diatom abundance that were elevated relative to other locations during the SW Monsoon. The SW Monsoon was the most productive period, but SW Monsoon primary productivity values were lower than predicted because efficient grazing by mesozooplankton kept diatoms from accumulating the biomass necessary for achieving the high levels of primary productivity characteristic of other coastal upwelling regions. The high rates of chlorophyll-specific productivity ($P^{B}_{opt} > 10$ mmol C mg Chl^{-1} d^{-1}) observed in the 1995 SW Monsoon, together with the observed dust flux and iron concentrations, indicate that the Arabian Sea was more iron replete than the equatorial Pacific Ocean or the Southern Ocean.

1. Introduction

"There is no better place on earth to study the reaction of an ocean with the atmosphere than the northern Indian Ocean," according to Dietrich (1973). However, as Wüst (1959) emphasized, to resolve the response of the ocean and its biota to the strong, seasonally reversing monsoonal wind, "a schematic grid system of sections with repeated observations in different seasons" is needed. The US JGOFS Arabian Sea Expedition followed the advice of Wüst (1959) in that repeated observations were made at the same locations in the Arabian Sea in different seasons throughout the year (Smith et al., 1998a). The goals of JGOFS are (1) to determine and understand processes controlling the time-varying fluxes of carbon and associated biogenic elements; and (2) to predict the response of marine biogeochemical processes to climate change. The primary productivity analyses carried out during the Arabian Sea Expedition and described here contribute to the achievement of the first JGOFS goal.

The overall science plan of the US JGOFS Arabian Sea Expedition (Smith, 1991) and the specific plan of the primary productivity work were based on the conventional wisdom concerning physical and biological variability of the Arabian Sea. Defining characteristics of the Arabian Sea seasonal cycle of physical conditions are (1) strong wind stress during the SW Monsoon that results in widespread upwelling and mixing in the boreal summer; (2) moderate strength, relatively cool and dry winds during the winter NE Monsoon that promote evaporative cooling, forcing strong convective mixing in the offshore region; and (3) during the Spring and Fall Intermonsoon transition periods, weak winds and surface layer heating that produce strong stratification, shallow mixed layers (MLs) and oligotrophy.

The regularity and strength of the monsoon wind and current reversals have been known since the 10th century. In particular, the SW (or summer) Monsoon, which begins in June and ends abruptly some time between the end of August and mid-September, has long held the attention of society because it brings essential rains to the Indian subcontinent. Because of this societal link the

timing and strength of the SW Monsoon have been recorded for centuries. The SW Monsoon starts rapidly and regularly. In the Arabian Sea, it not only forces upwelling of nutrient-rich subsurface water, but also provides a high flux of iron-rich eolian dust to a tropical ocean that receives intense (saturating) solar radiation. These favorable conditions are maintained throughout the 3- to 3.5-month period of the SW Monsoon, resulting in a sustained high rate of primary productivity that is exceptional in its magnitude among offshore ocean regions (Ryther and Menzel, 1965; Zeitzschel, 1973; Yoder et al., 1993). The processes responsible for this sustained high primary productivity during the SW Monsoon are strong and continuous upwelling (Currie et al., 1973; Smith and Bottero, 1977; Brock et al., 1992), high subsurface nutrient concentrations (Ryther and Menzel, 1965; McGill, 1973), and high eolian iron supply through dust (Bauer et al., 1991; Smith, 1991).

Upwelling and nutrient enrichment resulting from the strong SW Monsoon and the associated high rates of primary productivity have been known for many years (Ryther and Menzel, 1965; Ryther et al., 1966; Kabanova, 1968; Aruga, 1973; Krey, 1973; Krey and Babenerd, 1976; Qasim, 1977; Nair and Pillai, 1983). While there are no annual time series per se, there were enough observations for Longhurst (1998) to propose a conceptual model of the annual productivity cycle that ranges from $> 250\,\mathrm{mmol\ C\,m^{-2}\,d^{-1}}$ during the SW Monsoon to $\approx 60\,\mathrm{mmol\ C\ m^{-2}\,d^{-1}}$ during the remainder of the year.

The strong seasonal cycle in nutrient supply, alternating between highly eutrophic and moderately oligotrophic conditions, was assumed to provide a temporal pattern that makes the Arabian Sea uniquely valuable for testing hypotheses dealing with the onset, maintenance and decay of high productivity and export of organic material to the deep sea (Nair et al., 1989). In addition, the Arabian Sea was thought to have very strong spatial gradients in primary productivity during the SW Monsoon, with exceptionally eutrophic conditions in the Omani coastal region changing to oligotrophic conditions in the central portion of the Arabian Sea along 65°E (Smith, 1991). The temporal and spatial patterns of primary productivity variability were assumed to result directly from monsoonal forcing of the upper ocean (Bartolacci and Luther, 1999). The Arabian Sea Process Study Science Plan (Smith, 1991) described the overriding hypothesis of the primary productivity effort as follows: *"Does the regularity of monsoon reversals and strength of monsoon forcing create conditions in which the response of the region in terms of carbon fixation (primary production) is immediate and massive and in which balances between carbon and nitrogen exchanges between the euphotic zone and the atmosphere and euphotic zone and depth are predictably time-varying signals of large magnitude?"* Therefore, the primary objective of this study was to test the hypothesis *that monsoonal wind variability forces highly eutrophic conditions ($> 250\,\mathrm{mmol\ C\,m^{-2}\,d^{-1}}$) during the SW Monsoon and moderately oligotrophic conditions ($\approx 60\,\mathrm{mmol\ C\,m^{-2}\,d^{-1}}$) during the remainder of the year.*

In the Arabian Sea, seasonal variability in two properties – nutrients and ML depth – exceeds by several fold the range of variability found in other tropical regions; at the same time, the range of variation in two other properties that force productivity – solar radiation and sea-surface temperature – is similar to that found in other tropical regions (Longhurst, 1993, 1995). In most oceanic regions deep MLs are confounded by low incident solar radiation (E_0) and seasonally minimal temperatures, so it is difficult to assign causality to the specific physical process limiting photosynthetic productivity. In strong contrast, in the Arabian Sea deep MLs occur in combination with relatively high sea-water temperatures and high E_0 (Marra et al., 1998). This unique combination of

productivity forcing (high light and temperature with deep ML) creates a natural experiment on the regulation of primary productivity; therefore, the primary productivity work tested a second hypothesis, *that deep mixing, per se, limits primary productivity and photosynthetic performance in offshore regions of the Arabian Sea.*

In addition to the strong seasonal variability of reversing monsoonal winds, the northern Arabian Sea has a spatial wind pattern that exists in no other ocean (Smith and Bottero, 1977). During the SW Monsoon (from June to mid-September) there are, close to the Omani coast, alongshore winds that favor upwelling along the coast; seaward of the coast, winds intensify to an exceptionally strong offshore maximum commonly called the "Findlater Jet." ("Findlater Jet" is the name properly given to the high wind feature at 1 km altitude (Findlater, 1971), while the surface expression of this unique wind feature is properly called the "Somali Jet." Oceanographers frequently, but incorrectly, use "Findlater Jet" to refer to the surface wind feature.) Seaward of the wind jet, decreasing southwesterly wind speeds cause negative wind-stress curl (Hastenrath and Lamb, 1979; Halpern and Woiceshyn, 1999), which drives strong Ekman pumping that deepens the surface ML considerably (Luther, 1987; Bauer et al., 1991; Brock et al., 1991; Brock and McClain, 1992; McCreary et al., 1996). Fig. 1 shows the regions where these models predict dramatic ML deepening forced by the negative wind-stress curl of the spatially constrained Findlater Jet. In observations, the jet continuously meanders northward and southward of the mean position (Fig. 1) at frequencies of a few days. This time-dependent spatial variability means that the Arabian Sea region around the Findlater Jet is forced not with constant positive (or negative) curl, as in the models, but with a positive (or negative) curl that reverses every few days. This apparent difference between model predictions and the actual Arabian Sea patterns heightened interest in looking for the predicted Ekman-driven ML deepening and its biological consequences: light limitation and reduced photosynthetic performance (Sverdrup, 1953; Smetacek and Passow, 1990; Bartolacci and Luther, 1999).

The geographically distinct regions of upward and downward vertical velocities at the bottom of the Ekman layer, if present in the ocean, provide a setting for testing the connection between ML depth and phytoplankton sinking (Smayda and Boleyn, 1965; Smayda, 1970; Smetacek, 1980). The ML depth/sinking connection is based on the hypothesis that when phytoplankton, especially large diatoms, are subjected to deep mixing, light limitation reduces photosynthetic performance to the degree that the phytoplankton are not able to produce enough reducing power to fuel the active transport necessary to move heavy ions out of the cell and maintain cellular buoyancy (Gross and Zeuthen, 1948; Waite et al., 1992). In a region of Ekman pumping and ML deepening, phytoplankton would be expected to have reduced photosynthetic performance because of both light and nutrient limitation (Bauer et al., 1991; Banse and English, 2000). Thus, the primary productivity work reported here tested a third hypothesis, *that Ekman pumping, ML deepening and subsequent decreased photosynthetic performance occur in the region south of the Findlater Jet, creating a strong spatial gradient of high productivity inshore of the jet and very low productivity offshore of it in the negative-curl region.*

The physical and chemical observations of the 1995 Arabian Sea Expedition have shown that monsoonal variability dominates the physical and chemical dynamics of the upper ocean. In keeping with the suggestion made by Dietrich (1973), this region is a good location to determine how physical forces drive the biological response of the pelagic community. Despite documented interannual variation (Brock and McClain, 1992; Halpern and Woiceshyn, 1999), the SW

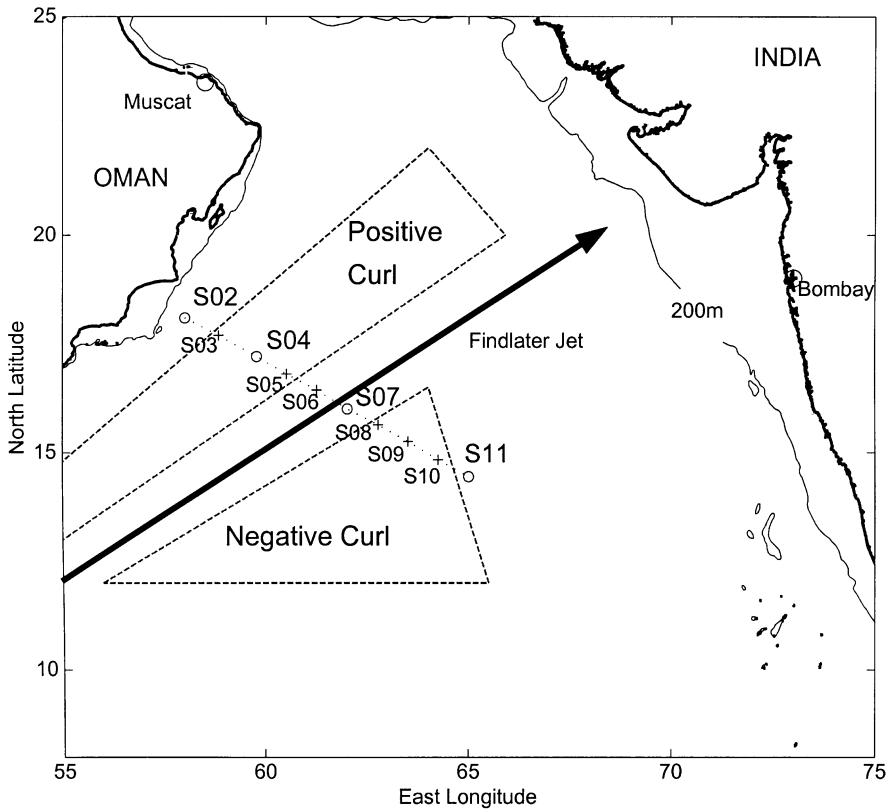

Fig. 1. Map of the study area showing the southern section of the US JGOFS cruise track (for the position of the northern line and offshore stations, see Smith et al., 1998). The distance from the coast to S11 was about 1000 km; the section was always run from S11 to S02. Open circles show the position of the long stations where both in situ and on-deck primary productivity incubations were carried out; crosses show the position of the stations where only on-deck incubations were carried out. Also shown are the regions assumed to have positive and negative wind-stress curl, as delimited by Brock et al. (1991), and the 1995 observed mean position of the Findlater Jet (Smith et al., 1998).

Monsoon cycle is one of the world's most regular atmospheric phenomena (Fieux and Stommel, 1977); but was 1995 a typical year in terms of wind stress and heat exchange? Monthly mean values indicate that 1994/1995 was typical in timing of the seasonal progression of wind stress and heat exchange (Halpern et al., 1998; Weller et al., 1998). At higher temporal resolution, however, the 1995 SW Monsoon onset in 1995 was 7 – 10 days later than in the preceding and following years (Weller et al., 1998; Halpern and Woiceshyn, 2001). During July 1995, the strength of the monsoonal winds in the region of the southern section was 10% less than the 1988–1997 climatology; during August, the difference was less than 10%; and during September, the winds were about equal to the climatological mean (Halpern and Woiceshyn, 2001). During the March and April 1995 Spring Intermonsoon, winds were moderate ($\approx 4.0\,\mathrm{m\,s^{-1}}$), but this value was about 40% higher than the 1911–1970 climatological Spring Intermonsoon mean ($2.5\,\mathrm{m\,s^{-1}}$) (Smith et al., 1998b).

The NE Monsoon period in the northern Arabian Sea in 1995 was a period of steady and moderate winds, clear skies, low humidity and heat loss from the ocean to the atmosphere; in contrast, the SW Monsoon was a period of strong winds, more or less continuous cloud cover, high humidity and heat gain by the ocean (Smith et al., 1998a). During the NE Monsoon evaporative cooling of the Arabian Sea both decreased the upper-layer seawater temperature and increased the salinity; this produced dense water that was convectively mixed, resulting in deep MLs (Weller et al., 1998). The convective mixing eroded into the nutricline, bringing moderately high concentrations of nutrients to a large area of the offshore region. The only portion of the study area not undergoing convective mixing during the NE Monsoon was the region adjacent to the coast of Oman (Morrison et al., 1998). During the Spring and Fall Intermonsoon periods the MLs were very shallow, stratification was strong, and nutrient concentrations were low over the entire study area (Morrison et al., 1998).

During the SW Monsoon there was evidence of strong upwelling with cool, lower salinity, nutrient-rich water in the inshore region adjacent to Oman (Lee et al., 2000; Shi et al., 2000). The inshore coastal upwelling region was similar in both hydrography and nutrients to the four other major coastal upwelling regions (Barber and Smith, 1981). As in other coastal upwelling regions, temperature increased and nutrients decreased along the US JGOFS southern section from inshore to offshore. However, the spatial domain over which nutrients were enriched was much larger in the Arabian Sea. In the Peru coastal upwelling, high nutrient water reaches offshore 100 km or less, while off California and Northwest Africa the offshore extent of upwelled water is 200 km or less (Barber and Smith, 1981). In contrast, the offshore extent of high-nutrient water during the SW Monsoon was 500–700 km (Morrison et al., 1998). As is common in coastal upwelling systems, the Arabian Sea during the SW Monsoon was also characterized by strong, narrow jet-like currents that ran in a generally offshore direction from the zone of coastal upwelling to about 700 km offshore (Brink et al., 1996). In addition, there were numerous well-defined mesoscale eddies that generated considerable variability in hydrographic properties (Flagg and Kim, 1998; Lee et al., 2000). Filaments and eddies dominated the velocity field in this region during the SW Monsoon. There was surprisingly little organized offshore flow despite evidence of strong onshore/offshore gradients in hydrographic properties. Mean flow in the region of the US JGOFS southern section was to the southwest except for the coastal upwelling zone within 150 km of the coast where the flow was to the northeast (Flagg and Kim, 1998).

The Arabian Sea Expedition combined six process cruises throughout the annual cycle, a fixed station grid, interdisciplinary research teams, moorings and satellite coverage. Rarely has such an intense effort been focused on a single oceanic region. An overview of the program and papers describing its findings are given in *Deep-Sea Research II* Vol. 45, No. 10–11 (1998); Vol. 46, No. 8–9 (1999); and Vol. 47, No. 7–8 (2000): all three edited by S. L. Smith (Smith, 1998, 1999, 2000).

2. Methods

2.1. Research plan

This paper presents observations from the six Arabian Sea Expedition process cruises (Table 1). While the expedition occupied two sections that extended offshore about 1000 km, a collection of

Table 1
US JGOFS 1995 Arabian Sea Expedition cruises and the individuals who carried out the primary productivity observations

Cruise No.	Cruise name	Season	Cruise duration	Date at S07	Prim. prod.team
TN043	P1	NE Monsoon (Jan)	08 Jan–05 Feb	23–24 Jan	John Marra Carol Knudson Steve Lindley
TN045	P2	Spring Intermonsoon	07 Mar–04 Apr	30–31 Mar	John Marra Carol Knudson Mike Hiscock
TN049	P4	SW Monsoon (mid)	17 Jul–15 Aug	03–04 Aug	Richard Barber Carol Knudson Elaine Barber
TN050	P5	SW Monsoon (late)	18 Aug–15 Sep	04–05 Sep	Richard Barber Fei Chai Elaine Barber
TN053	P6	Fall Intermonsoon	29 Oct–26 Nov	15 Nov	John Marra Zackary Johnson
TN054	P7	NE Monsoon (Dec)	30 Nov–29 Dec	17–18 Dec	Carol Knudson Zackary Johnson

nine offshore stations and a few inshore stations on the Omani shelf, the in situ primary productivity stations were concentrated on the southern section of the US JGOFS cruise track (Fig. 1). Therefore, this paper is limited to results from stations along the 1000-km southern section (Stations S02–S11), from the coast of Oman to the center of the Arabian Sea at 65°E. This southern section crosses the western half of the Arabian Sea where the SW and NE Monsoons drive dramatic seasonal variability. In this portion of the Arabian Sea (Fig. 1), the US JGOFS cruises carried out dense seasonal sampling of primary productivity (Table 2) and related atmospheric, physical, chemical and biological properties. Offshore stations along 65°E from 20°N–10°N are not included in this analysis because of their location in a permanently oligotrophic region (Longhurst, 1993, 1995, 1998; Smith et al., 1998a). The inshore station S01 was not included in this paper because in situ primary productivity observations were made there infrequently.

The six process cruises were scheduled throughout 1995 to resolve seasonal patterns. The 1995 SW Monsoon was sampled by two consecutive cruises (TN049 and TN050). The NE Monsoon was sampled in two separate winters: TN043 took place during the 1994/1995 NE Monsoon in January 1995; TN054 was carried out during the 1995/1996 NE Monsoon in December of 1995. The research plan placed 10 stations along the 1000-km section to resolve onshore/offshore gradients. The inshore end of the section (Station S02) was 150 km off the coast of Oman; the offshore end (Station S11) was in the central Arabian Sea. The stations occupied were of three different durations–short, intermediate and long (Smith et al., 1998a). The long stations were 2.5–3 days in duration. At long stations (S02, S04, S07 and S11 in Fig. 1), both in situ and on-deck (simulated in situ) primary productivity incubations were carried out; at short and intermediate stations (Fig. 1) only on-deck incubations were carried out. The on-deck primary productivity incubations were "ground-truthed" with in situ results (Fig. 2) as described in Barber et al. (1997). At stations where

Table 2
In situ (boldface) and on-deck (regular font) integrated primary productivity, surface chlorophyll and specific productivity (P^B_{opt}) at each station on the southern transect from S02 to S11. P^B_{opt} is the highest water column productivity in a 24-h on-deck incubation normalized by chlorophyll concentration at the depth of the highest water column productivity. Bracketed values at S10 are interpolated from neighboring stations of P5 (Late SW Monsoon). Values in parentheses are standard errors of the annual mean calculated from the seasonal means

Station	NE Monsoon Jan	Intermonsoon spring	SW Monsoon		NE Monsoon	
			Mid	Late	Dec	Mean ± SE
Primary Productivity (mmol C m^{-2} d^{-1})						
S02	**121**	**71**	**81**	**92**	**76**	**88 ± 9**
S03	150	87	135	93	87	111 ± 13
S04	**85**	**101**	**118**	**72**	**78**	**91 ± 8**
S05	201	65	99	99	83	109 ± 24
S06	123	105	132	119	121	120 ± 4
S07	**100**	**80**	**134**	**147**	**85**	**109 ± 13**
S08	145	79	183	181	89	135 ± 22
S09	202	**92**	158	70	79	120 ± 26
S10	154	112	184	[99]	90	128 ± 18
S11	**84**	**71**	**129**	**127**	**96**	**101 ± 12**
Mean ± SE	137 ± 13	86 ± 5	135 ± 10	110 ± 11	88 ± 4	111 ± 11 (5)
Surface Chlorophyll *a* (mg m^{-3})						
S02	**0.78**	**0.16**	**0.35**	**0.56**	**0.51**	**0.47 ± 0.10**
S03	1.06	0.17	0.56	0.47	0.41	0.54 ± 0.15
S04	**0.29**	**0.23**	**0.39**	**0.57**	**0.47**	**0.39 ± 0.06**
S05	0.28	**0.13**	0.44	0.84	0.68	0.47 ± 0.13
S06	0.40	0.20	0.74	0.61	0.49	0.49 ± 0.09
S07	**0.38**	**0.19**	**0.44**	**0.51**	**0.43**	**0.39 ± 0.05**
S08	0.39	0.09	0.65	1.31	0.47	0.58 ± 0.20
S09	0.44	0.13	0.6	0.47	0.33	0.39 ± 0.08
S10	0.5	0.09	1.08	[0.47]	0.35	0.50 ± 0.16
S11	**0.28**	**0.08**	**0.52**	**0.48**	**0.36**	**0.34 ± 0.08**
Mean ± SE	0.48 ± 0.08	0.15 ± 0.02	0.58 ± 0.07	0.63 ± 0.08	0.45 ± 0.03	0.46 ± 0.08 (0.02)
Specific Productivity (P^B_{opt}) (mmol C mg Chl^{-1} d^{-1})						
S02	**8.24**	**7.49**	**12.20**	**7.75**	**5.78**	**8.29 ± 1.06**
S03	10.54	9.58	14.10	7.00	6.29	9.50 ± 1.39
S04	**9.58**	**10.80**	**11.55**	**15.57**	**6.45**	**10.79 ± 1.48**
S05	8.23	6.32	10.70	7.41	8.11	8.15 ± 0.72
S06	17.79	6.14	10.01	7.37	6.14	9.49 ± 2.19
S07	**9.05**	**10.13**	**10.47**	**16.39**	**11.44**	**11.50 ± 1.28**
S08	10.58	12.40	15.13	14.72	9.37	12.44 ± 1.13
S09	16.32	**11.56**	15.28	8.34	10.20	12.34 ± 1.51
S10	9.76	20.81	14.68	[12.76]	12.16	14.03 ± 1.87
S11	**8.65**	**10.06**	**7.89**	**17.18**	**7.54**	**10.26 ± 1.78**
Mean ± SE	10.87 ± 1.07	10.53 ± 1.32	12.20 ± 0.79	11.45 ± 1.34	8.35 ± .73	10.68 ± 0.65 (0.60)

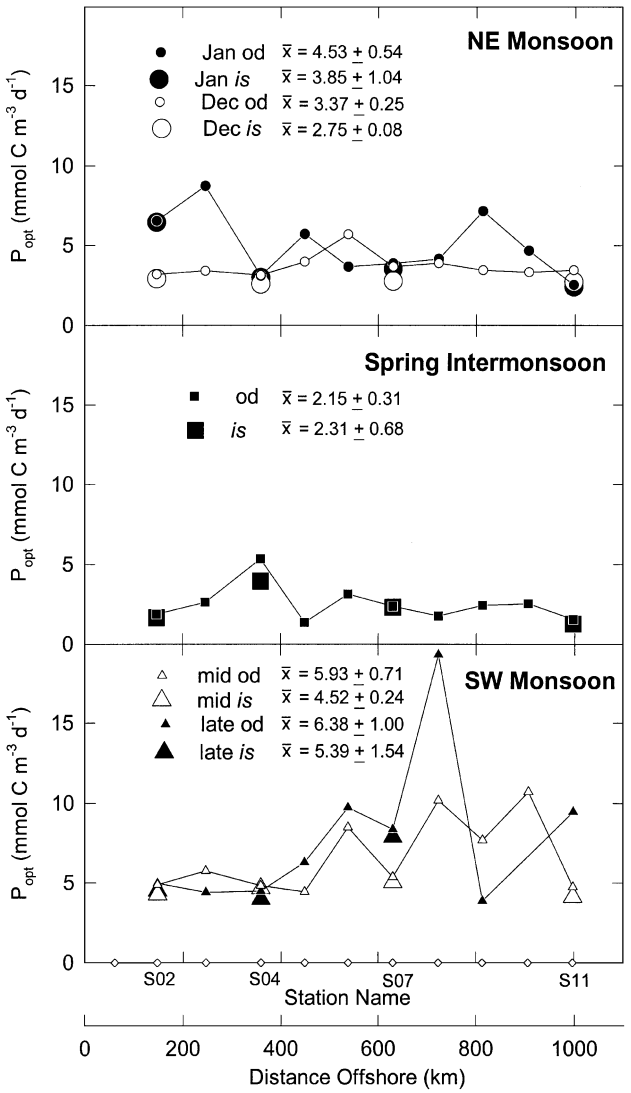

Fig. 2. P_{opt}, the highest water column productivity in 24-h in situ (*is*) and 24-h on-deck (od) incubations, versus distance offshore on the southern section from S02 to S11 during three seasons.

both on-deck and in situ observations were made, results agree well (Fig. 3). On five of the cruises (TN043, TN045, TN049, TN050 and TN054) (Table 1) the same long, in situ stations and the same short and intermediate stations were occupied, with two exceptions: at Station S11 of TN050 strong wind prevented deployment of the in situ incubation array, so only on-deck incubations were carried out; at Station S10 of TN050 high winds prevented all over-the-side work. Primary productivity and chlorophyll *a* values for S10, therefore, were interpolated from the neighboring stations, S09 and S11.

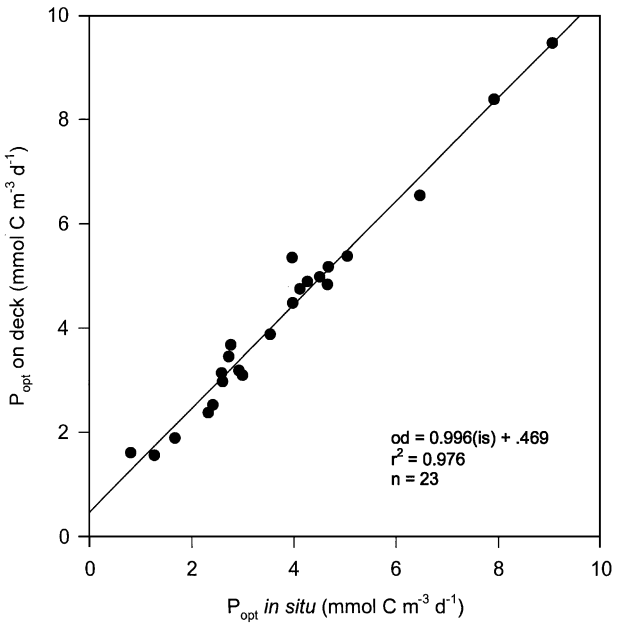

Fig. 3. A scatter plot of P_{opt}, the highest water column productivity in a 24-h incubation, showing in situ (*is*) versus on-deck (od) incubations, for six process cruises at the four long stations (S02, S04, S07 and S11) where both incubations were carried out.

The Fall Intermonsoon cruise (TN053) had a different scientific objective from the other five process cruises, so it followed an opportunistic cruise track and did not always sample the standard station locations (Smith et al., 1998a). The four standard locations on the southern section that were sampled on the Fall Intermonsoon cruise are included in the figures; however, because sampling of the southern section was so sparse, the Fall Intermonsoon values are not included in calculations of annual means.

2.2. Physical and chemical observations

Continuous wind, air and subsurface temperature, and upper-ocean current measurements were made at a surface buoy moored at 15.5°N, 61.5°E (Weller et al., 1998). To obtain three-dimensional resolution of the physical fields in the vicinity of the US JGOFS southern section, a SeaSoar towed-array was employed on cruises carried out by the US Office of Naval Research (ONR) Forced Upper Ocean Dynamics project (Smith et al., 1998a; Lee et al., 2000).

Vertical profiles of nutrients, salinity and temperature were recorded at each station (Morrison et al., 1998; Gardener et al., 1999) using a dual sensor (temperature and salinity) Seabird CTD system equipped with a SeaBird carousel water sampler. Nutrient analyses were done as prescribed in the JGOFS Protocols (SCOR, 1996), which are available at http://www1.whoi.edu/jgofs.html. Since new nutrients (Dugdale and Goering, 1967) – nitrate, phosphate and silicic acid – usually covaried in this study, nitrate is used to represent all of the new nutrients. The only exception to this

rule occurred in the current filament at Station S08 during the late SW Monsoon. Minor procedural differences in the nutrient analyses are noted in the "Readme" files attached to the US JGOFS nutrient data files. Analysis of ammonium concentration was done with the Berthelot reaction using a slight modification of the method described by Whitledge et al. (1981).

In this analysis, ML depth was defined as the depth at which subsurface σ_θ differed from surface σ_θ by 0.013. The conductivity, temperature and depth (CTD) casts used to calculate ML depth were taken at the same time as sampling for primary productivity determinations (between 2300 and 0200). The equations of Stommel (1965) were used to calculate vertical velocity at the base of the Ekman layer (W_{EK}) from observations of wind-stress curl. Scatterometer measurements recorded by the first European Remote-Sensing Satellite (ERS–1) were used to estimate wind-stress curl at $1^\circ \times 1^\circ$ intervals throughout the Arabian Sea (Halpern et al., 1998). The W_{EK} calculation used wind-stress curl averaged over 2–3 inertial periods.

2.3. *Chlorophyll* a *and other pigments*

Chlorophyll *a* was determined both fluorometrically and by high-performance liquid chromatography (HPLC) at all stations and all depths of each of the process cruises. Using a Turner Designs Model 10–AU fluorometer, fresh samples were extracted in 90% acetone at -20°C for 24–30 h (Venrick and Hayward, 1984). Other than this modification of extraction procedure, the method used was the conventional fluorometric procedure of Holm-Hansen et al. (1965) and Lorenzen (1966). Plant pigments, including chlorophyll *a,* for TN043, TN049 and TN054 were analyzed by HPLC following the procedures described in Goericke and Repeta (1993); for TN045, TN050 and TN053, procedures are described in Latasa and Bidigare (1998). Intercalibrations show that these two HPLC procedures gave equivalent results.

As shown in Fig. 4, fluorometric and HPLC determinations of chlorophyll *a* usually agreed well during the Arabian Sea cruises, but they disagreed during the SW Monsoon period when significant quantities of non-photosynthetic chlorophyll were present. The fluorometrically determined chlorophyll *a* concentrations at Stations S05 to S11 on the late SW Monsoon cruise (TN050) overestimated photosynthetically active chlorophyll *a* (Sathyendranath et al., 1999). This overestimation resulted from the inability of the fluorometric method to distinguish between chlorophyll *a* (monovinyl and divinyl chlorophyll *a*) and chlorophyllide *a* (dephytolated monovinyl chlorophyll *a*, which is a monovinyl chlorophyll *a* degradation product). Chlorophyllide *a* is present in senescent diatoms because of the elevated chlorophyllase activity present in these photoautotrophs (Jeffrey, 1974; Trees et al., 1985). The presence of senescent diatoms in the gelatinous matrix of co-occurring *Phaeocystis* colonies at these stations was confirmed by microscopic observations (Garrison et al., 1998). In this report, therefore, chlorophyll *a* concentrations determined by HPLC were used for Stations S05 to S11 for the late SW Monsoon period.

Surface chlorophyll *a* ($\approx$ ML chlorophyll *a*) rather than integrated euphotic zone chlorophyll *a* is used as a diagnostic property in this analysis for several reasons. First, the integrated euphotic zone chlorophyll *a* concentration does not reflect the concentration of active pigments when a deep chlorophyll maximum is present at the base of the euphotic zone where only a small percent of the total primary productivity takes place. Second, chlorophyll *a* concentration per unit volume is a diagnostic that is interpretable per se; for example, a chlorophyll *a* concentration of 1.5 mg m^{-3} conveys information, while an integrated value of 15 mg m^{-2} can be a high or low

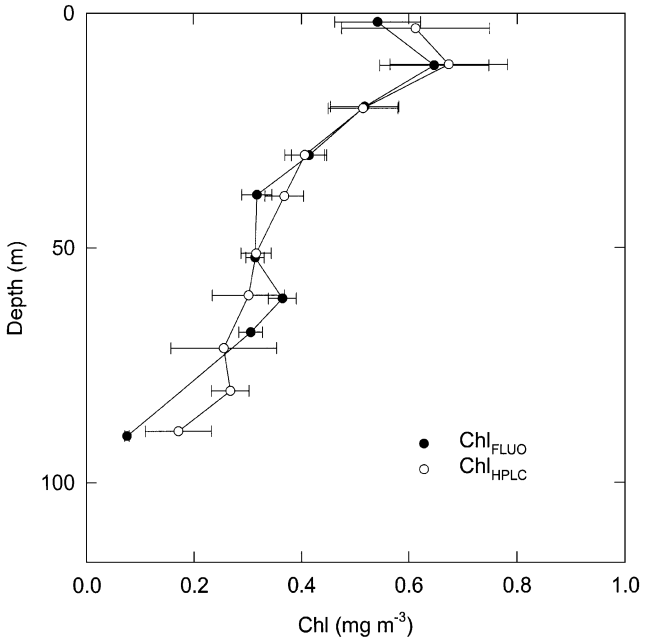

Fig. 4. Chlorophyll *a* concentration by the fluorometric method (Holm-Hansen et al., 1965; Lorenzen, 1966) versus the HPLC method (Goericke and Repeta, 1993) on the TN043 cruise, with the mean and standard error for all stations.

concentration depending on the depth of the euphotic zone. Finally, the surface chlorophyll *a* concentration is the property measured by satellite, and in the Arabian Sea most of the knowledge of seasonal and temporal patterns of phytoplankton abundance is based on satellite observations (Banse and English, 1994 and 2000).

2.4. Primary productivity

Odum (1971) defines *primary productivity* as "the rate at which energy is stored by the photosynthetic and chemosynthetic activity of producer organisms in the form of organic substances which can be used as food materials." This definition is conceptually powerful, but as an operational definition it is flawed because it is difficult to measure in assemblages of natural plankton, particularly with tracer methods. A property that can be determined rapidly with considerable precision using ^{14}C uptake is *net daily community particulate primary productivity* (Richardson, 1991; Williams, 1993a, b). Disadvantages of this property (as determined by ^{14}C uptake) are that it is only one component of photosynthetic production because it does not measure dissolved organic productivity (Williams, 1995; Hansell and Carlson, 1998) and it refers not to a single autotrophic process of phytoplankton, but to the net sum of a variety of autotrophic and heterotrophic processes carried out by a community of phytoplankton, bacteria and protozoans (Williams, 1981; Bender et al., 1987; Williams and Lefevre, 1996; Bender et al., 1999; Robinson and Williams, 1999; Laws et al., 2000; Dickson et al., 2001). Advantages of using *net daily community particulate primary productivity* (as determined by ^{14}C uptake) are that it has a widely accepted operational definition (Peterson, 1980; Williams, 1993b); it has a strong and causal correlation to a variety of biological,

chemical and geochemical processes of interest to oceanographers and geoscientists outside the subdiscipline of phytoplankton physiology (Suess, 1980; Pace et al., 1987; Iverson, 1990; Wassman, 1990; Bertrand and Lallier-Verges, 1993); and it covaries with the process captured in the Odum (1971) definition (Laws, 1991; Laws et al., 2000). In a symposium volume that discusses the issue of measured properties versus conceptual definitions of primary productivity, Li and Maestrini (1993) recommended using the term *primary productivity* to denote that property which is measured by the ^{14}C uptake method; for the remainder of this report we use *primary productivity* as they recommended.

Methods for determining daily *in situ* primary productivity have converged considerably in US JGOFS and other recent work. The in situ procedure used in the US JGOFS Arabian Sea Expedition is similar to those used by Karl et al. (1990) in the Hawaiian Ocean Time Series (HOT), Lohrenz et al. (1992) and Malone et al. (1993) in the Bermuda Time Series (BATS), Chipman et al. (1993) and Martin et al. (1994) in the North Atlantic Bloom Experiment (NABE), Welschmeyer et al. (1993) in the Subarctic Pacific Ecosystem Research (SUPER) project, Barber et al. (1996) in the Equatorial Pacific Study (EqPac) and Smith et al. (in press) in the Antarctic Environment and Southern Ocean Process Study (AESOPS).

In the Arabian Sea Expedition, a Moss Landing Marine Laboratories trace-metal clean (TMC) rosette with General Oceanics Go-Flo™ sample bottles and a Kevlar cable (Sanderson et al., 1995; Hunter et al., 1996) was used for water collection on all six process cruises with the exception of the second half of the July/August mid-SW Monsoon cruise (TN049). Due to the loss of the TMC rosette midway through the TN049 cruise, an epoxy-coated rosette was used for the remainder of the cruise; a replacement TMC rosette was obtained for the remaining cruises. Samples for in situ and on-deck primary productivity determinations were collected between 0200 and 0300 hr from light depths corresponding to 93, 75, 55, 27, 15, 7, 4, 1 and 0.1% of the incident irradiance, E_0, as determined by a submarine quantum sensor (Biospherical Instruments, Inc., Model QSP-200) on the hydrographic cast made during the preceding afternoon at the same location (Morrison et al., 1998). For each depth sampled, six 280-ml polystyrene tissue culture flasks were filled and inoculated; four of the flasks were incubated in situ two on deck.

For in situ incubation, flasks were mounted on clear Plexiglas™ racks and, using conventional hydrowire clamps, each rack was attached to the array line at a position corresponding to the intended depth of incubation. The in situ primary production incubation array was launched before dawn so that the inoculated samples were exposed to a full, uninterrupted daily light period. After dark the array was picked up, the 12-h samples were immediately filtered and the remaining (24-h) samples were placed in on-deck incubators to complete their incubation through the dark period. The temperature regime of the on-deck incubators, cooled by surface sea water, was approximately the same as the in situ temperature profile because the MLs were relatively deep and below the ML the temperature gradient was relatively weak. During the daylight period the in situ incubation array was suspended from two floats, each with 30 kg of buoyancy, at the top of the 100-m array line, while a 25-kg weight at the bottom kept the line vertical in the water. A 20-m tag line connected the array line to a spar buoy equipped with a radar reflector, a flag, a xenon flasher and a VHF radio transmitter. During recovery of the array, once the tag line was caught with grapnel hooks, getting the array on deck took less than 30 min. The Plexiglas™ racks were unclamped as the array line was retrieved through the main stern A-frame. A complete description of the in situ procedure is given in Barber et al. (1996).

On-deck incubations were carried out in seawater-cooled, 40 cm × 20 cm × 30 cm Plexiglas™ incubator boxes. Light in the incubators was attenuated to 93, 75, 55, 27, 15, 7, 4, 1 or 0.1% E_0 by means of neutral density screening and blue Plexiglas™. Water for samples incubated in both the 93 and the 75% light level incubators was taken from the shallowest collection bottle. Autonomous recording thermometers monitored temperature in the incubators and incubator irradiance levels were checked weekly. Productivity values used in this paper are integrated to the 1% light depth, but both 1 and 0.1% light depth integration values are provided in the US JGOFS Data Management System. Integrations to the 0.1% light depth were on average only 3.5% higher than those integrated to the 1% light depth; more significantly, the portion of the photosynthetic profile from the 1% light depth to the 0.1% light depth shows very little spatial or temporal variation. Because this analysis focused on the factors forcing changes in primary productivity, the 1% integrations were analyzed. See Barber et al. (1997) for a description of the method used to estimate depths used in integration of carbon fixation in on-deck incubations.

Anhydrous crystalline sodium carbonate labeled with ^{14}C was added to a solution of 0.3 g of sodium carbonate in 1.0 l of Nanopure® water. The sodium ^{14}carbonate, obtained from New England Nuclear, had a specific activity of 55 mCi mmol^{-1}; the designation of this compound is NEC-088 H. Stock isotope solution was made up at 1-week intervals and stored at 4°C but allowed to come to ambient temperature before inoculation of the samples. The intended activity of the ^{14}C solution was 100 μCi ml^{-1}; however, total added activity was determined for each profile, so variations in added activity were adjusted in the calculation. Inoculation of 100 μl of ^{14}C solution was done with an Eppendorf disposable tip pipette. In addition to the two replicate samples incubated with ^{14}C solution, a third bottle was filled, inoculated with ^{14}C solution and immediately filtered to determine a time zero particulate ^{14}C blank as described by Huntsman and Barber (1977).

To determine the total added activity (DPM_{tot}), upon retrieval of incubation bottles a 1-ml subsample was taken from selected depths and added directly to scintillation vials containing 0.1 ml of beta-phenylethylamine (Iverson et al., 1976) and 1 ml of scintillation fluid. The samples were filtered through 25-mm Whatman GF/F filters with a 200-mmHg vacuum. The filters were sucked dry and placed flat in the bottom of a 20-ml scintillation vial, 0.5 ml of 0.5 N HCl was added, and the wetted filters were placed under a hood. After 24 h, a 1-ml volume of scintillation fluid was added and the filters were placed in the dark for a second 24-h period. The time zero particulate blanks, 24-h in situ samples and 1-ml subsamples for total activity were counted on the shipboard liquid scintillation counter. Counting efficiency for filters and total activity was determined by an internal ^{14}C toluene standard. Particulate carbon productivity for each in situ depth was calculated as follows:

$$PP = (DPM_{24} - DPM_0)(1.05)(2000\,\text{mmol}\,Cm^{-3})(DPM_{tot} \cdot \text{time})^{-1},$$

where $DPM_{24} = CPM_{24} \cdot \text{efficiency of filter counting}^{-1}$; CPM_{24} = counts collected on a GF/F filter after 24-h in situ incubation; $DPM_0 = CPM_0 \cdot \text{efficiency of filter counting}^{-1}$; CPM_0 = counts collected on a GF/F filter when sample was filtered immediately after the addition of ^{14}C carbonate solution; $DPM_{tot} = (CPM_{1\,ml} \cdot \text{efficiency of counting totals}^{-1}) \cdot \text{bottle volume in ml}$; CPM^{1ml} = counts in 1 ml of sample; 1.05 = factor for preferential uptake of ^{12}C over ^{14}C; 2000 = molarity in mmol m^3 of inorganic carbon in seawater.

Carbon-uptake rate per unit area for the water column down to the 1 and 0.1% light levels was calculated using a trapezoidal integration.

2.5. Photosynthetic performance

To characterize biomass-normalized photosynthetic performance this paper uses P^{B}_{opt}, the highest chlorophyll-normalized productivity value in a 24-h in situ or on-deck incubation. P^{B}_{opt} is operationally distinct from P^{B}_{max}, which is the maximal, chlorophyll-normalized, productivity value in a short (about 1-h) light-saturated, but not inhibited, incubation (Behrenfeld and Falkowski, 1997). Unlike P^{B}_{max}, P^{B}_{opt} may be light-limited, light-saturated or light-inhibited, depending on the in situ light field during the 24-h period when the estimate was made. P^{B}_{opt} is, more or less, an ecological property of the water column and its phytoplankton community, while P^{B}_{max} is an inherent physiological property of the ambient phytoplankton.

Primary productivity data for the Arabian Sea Expedition are available from the US JGOFS Data Management System at the US JGOFS Home Page http://www1.whoi.edu/jgofs.html.

3. Results

3.1. Wind stress and Ekman upwelling

Wind stress was highest during the SW Monsoon with values $> 0.2\,N\,m^{-2}$ offshore at Stations S07–S11. At the extreme offshore station, S11 (1000 km offshore), despite very high offshore wind stress and relatively deep mixing, the mixing was not deep enough to replace ML nutrients taken up by biological activity (Figs. 5 and 6). Both wind stress and ML depth were maximal at Station S11, but nitrate was reduced to the detection level.

The annual pattern of upwelling and downwelling at the bottom of the Ekman layer was calculated from the ERS-1 scatterometer wind fields (Halpern et al., 1998) for the four long in situ stations along the southern section (Fig. 7). The inshore station, S02 (147 km from the Omani coast), had significant Ekman upwelling ($> 0.25\,m\,d^{-1}$) during June, July and August in 1995. Farther offshore at Station S04, 359 km from the coast, there was no significant Ekman upwelling during the 1995 period of strong SW Monsoon winds, although temperature observations (Fig. 5) and nitrate concentrations (Fig. 6) indicate that the water at Station S04 had been recently upwelled or mixed from below. During the April/May 1995 period, just before onset of the SW Monsoon, there was Ekman downwelling across the southern section from Stations S02 to S07 (Fig. 7). At Station S07, 630 km off the coast, there was a downwelling pulse in May (early SW Monsoon) and a strong offshore upwelling pulse in July (mid-SW Monsoon). The Ekman upwelling estimates for June and July indicate that upwelling at Station S07 was spatially discontinuous from S02 upwelling; that is, significant Ekman upwelling was present at Station S07 but not at Station S04 (Fig. 7). An offshore source of ML nutrients that was discontinuous from the coastal source was further indicated by a second offshore peak in nitrate (Fig. 6) and other nutrients (Morrison et al., 1998). Station S07 was seaward of the mean axis of the Findlater Jet in 1995 (Fig. 1), but the time series of ML depth, Ekman upwelling and nitrate concentration (Fig. 8) show no evidence of the putative downwelling (Luther, 1987; Bauer et al., 1991; Bartolacci and Luther,

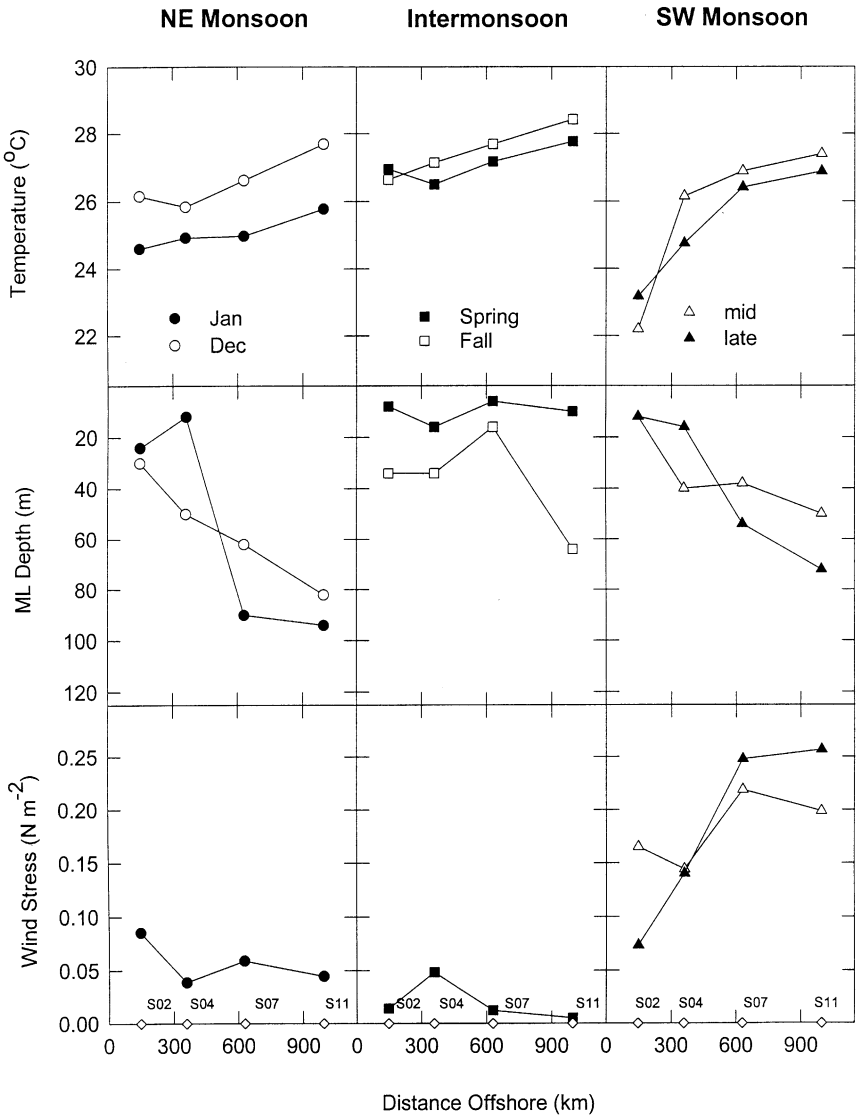

Fig. 5. Surface temperature, mixed-layer (ML) depth and wind stress versus distance offshore at the four long stations (S02, S04, S07 and S11) for three seasons. Mixed layer depth is defined as the depth at which subsurface σ_θ differed from surface σ_θ by 0.013. The meteorological mooring (Weller et al., 1998) was recovered in October 1995, so there are no wind stress estimates for the Fall Intermonsoon (TN053) or the December NE Monsoon (TN054). The S07 station values for the Fall Intermonsoon cruise (TN053) are means of adjacent stations because the S07 location per se was not occupied.

1999). Satellite temperature and acoustic Doppler current profiles (ADCP) show that the S07 region was the site of well-defined eddy and filament activity during the SW Monsoon (Flagg and Kim, 1998; Manghnani et al., 1998; Lee et al., 2000).

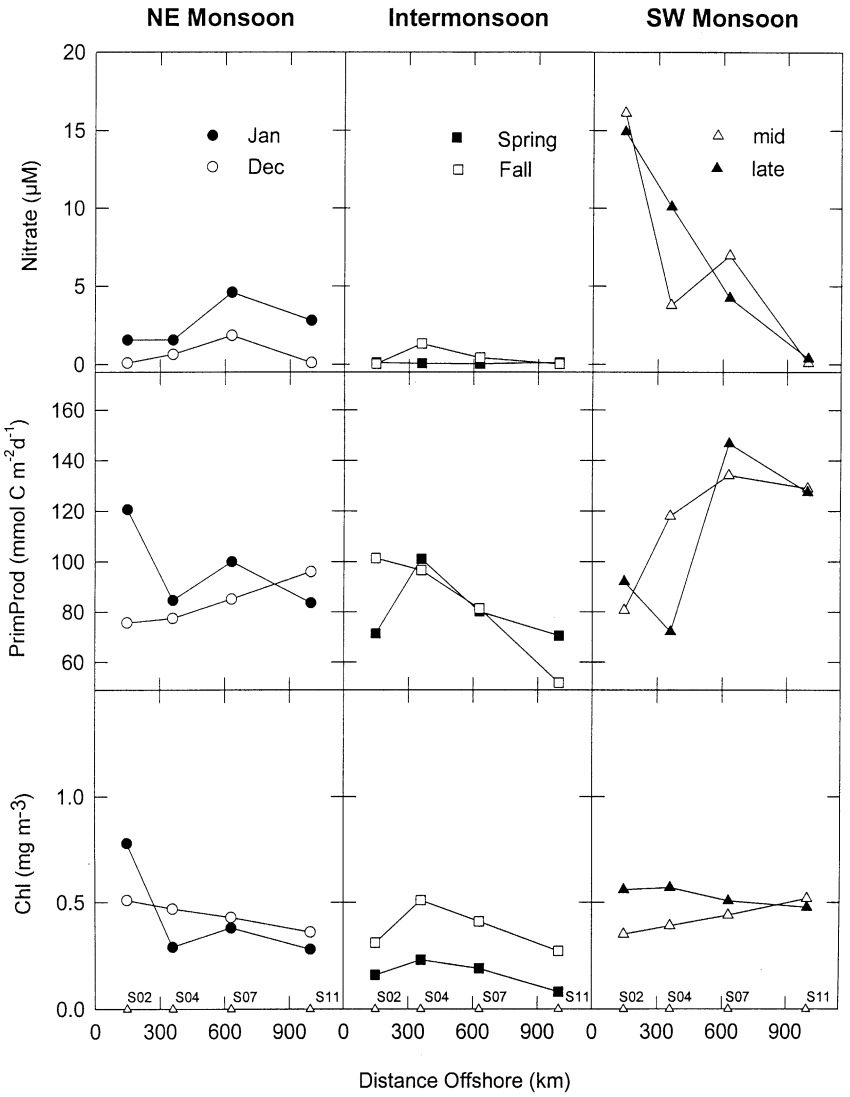

Fig. 6. Surface nitrate, primary productivity and surface chlorophyll *a* versus distance offshore at the four in situ stations (S02 to S11) for three seasons. The S07 station values for the Fall Intermonsoon cruise (TN053) are means of adjacent stations because S07 location per se was not occupied.

3.2. Physical response

Sections of temperature, ML depth, wind stress and surface nitrate (Figs. 5 and 6) show well-defined onshore/offshore gradients and seasonal differences. During the two intermonsoon seasons and the December 1995 NE Monsoon, surface temperatures of about 26°C inshore increased steadily offshore over the 1000-km section to > 28°C at the offshore location (Station S11). The January 1995 NE Monsoon had a similar gradient, but with an inshore value of 24.5°C

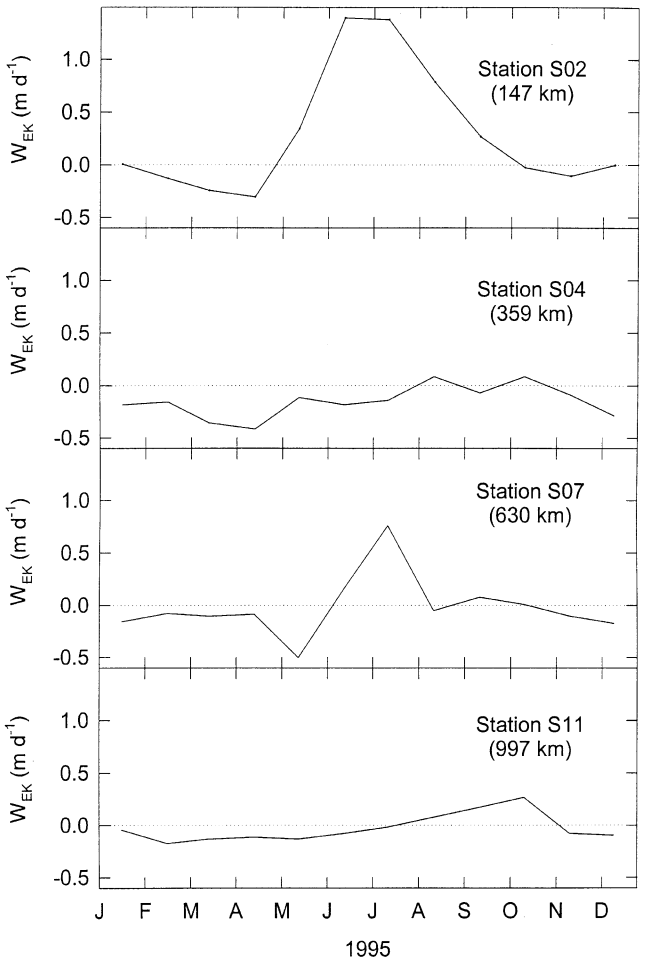

Fig. 7. The annual cycle of monthly mean Ekman upwelling and downwelling (W_{EK}) at the four in situ stations (S02–S11). (From Halpern et al., 1998).

and an offshore value of 26.0°C. During the SW Monsoon, values were 22.0–23.0°C inshore and > 27°C offshore.

During the Spring Intermonsoon, ML, defined as the depth at which subsurface σ_θ differed from surface σ_θ by 0.013, was very shallow (< 20 m) with no offshore gradient (Fig. 5). In each of the other periods there was an onshore/offshore gradient with ML depths of 12–34 m close to the coast and deepening offshore; the deepest MLs for each period were found about 1000 km offshore at Station S11. The offshore ML depth was 94 m during the January NE Monsoon and 82 m during the December NE Monsoon when winds were moderate in strength ($\approx 4\,\mathrm{m\,s^{-1}}$), but only 50 and 72 m during the mid- and late SW Monsoon when winds were much stronger ($\approx 12\,\mathrm{m\,s^{-1}}$) (Weller et al., 1998).

Low wind stress and increased seasonal heating during the Spring Intermonsoon produced the shallow ML depths during that period. During the January NE Monsoon, wind stress was higher

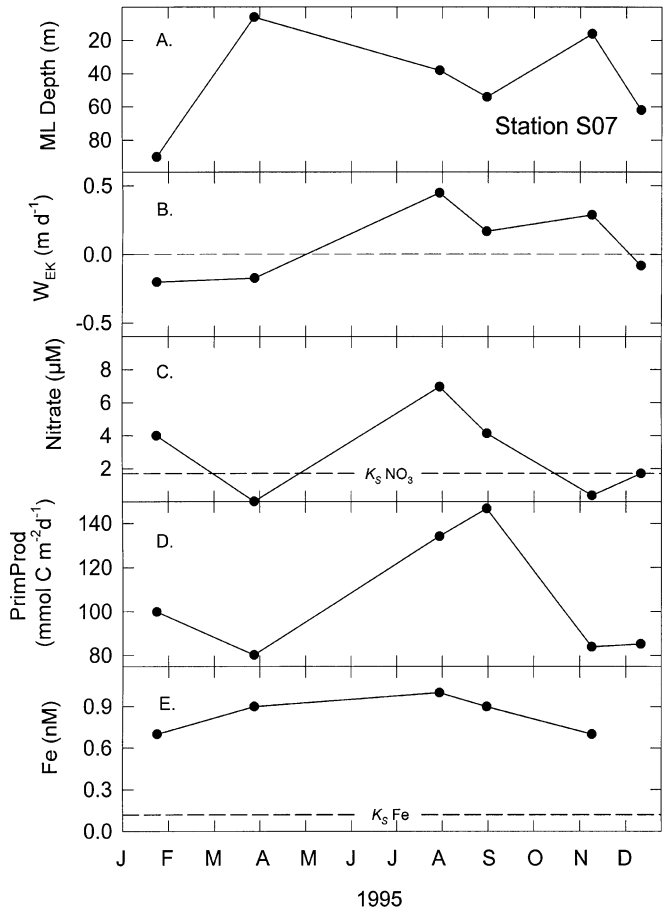

Fig. 8. Mixed-layer (ML) depth, Ekman upwelling and downwelling (W_{EK}), surface nitrate, integrated primary productivity and dissolved inorganic iron (Fe) observed when the five cruises were at S07. The station values for the Fall Intermonsoon cruise (early November, TN053) are means of adjacent stations because the S07 location per se was not occupied. The half saturation concentrations for nitrate (McCarthy et al., 1999) and iron (Coale et al., 1996a) are shown on their respective graphs by a dashed line. (W_{EK} from Halpern et al., 1998; Fe data from Measures and Vink, 1999).

than during the Spring Intermonsoon, but still relatively moderate at 0.04–0.08 N m^{-2} (Fig. 5). The deep January NE Monsoon MLs were accompanied by considerable seasonal cooling (Fig. 5) of the high-salinity offshore waters (Morrison et al., 1998).

3.3. *Primary productivity and chlorophyll* a *along the southern section*

Integrated primary productivity and surface chlorophyll *a* as functions of distance offshore during each cruise and each season are shown in Figs. 9 and 10. In contrast to temperature, ML depth, wind stress or nutrient concentration patterns, there is no consistent onshore/offshore gradient in either productivity or surface chlorophyll *a* during the SW Monsoon. Productivity and chlorophyll *a* patterns during the SW and NE Monsoons were characterized by a series of more or

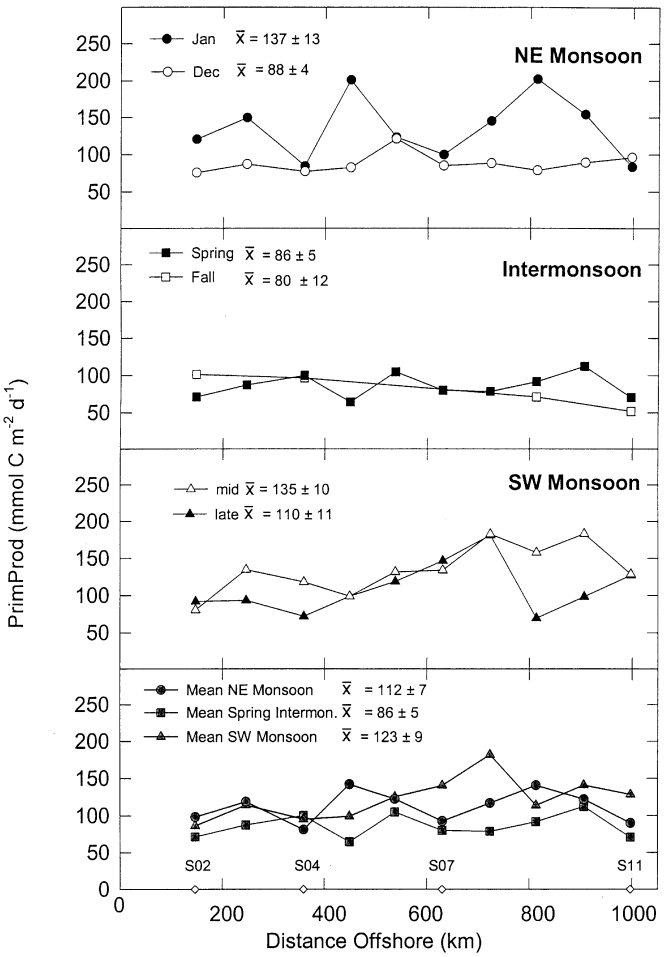

Fig. 9. Primary productivity, integrated to the 1% light depth, along the southern section from S02 to S11. The Fall Intermonsoon productivity (TN053, Table 1) is shown but not included in the mean in the bottom panel because only a few stations were occupied on the southern section during that cruise.

less isolated maxima (Figs. 9 and 10) along the 1000-km section, with the productivity maxima being almost three times the minima (202 versus 70 mmol $C\,m^{-2}\,d^{-1}$) (Table 3). During the highly productive January NE Monsoon and both SW Monsoon cruises, the highest primary productivity values were at stations on the offshore portion of the southern section (S08, S09 and S10), while the lowest productivity values on these three cruises were spread along the entire section (S02, S09 and S11) (Table 3).

Spring and Fall Intermonsoon periods had the lowest productivity and biomass (Figs. 9 and 10), but the mean Intermonsoon productivity values of 86 and 80 mmol $C\,m^{-2}\,d^{-1}$ for Spring and Fall, respectively, were surprisingly high (Fig. 9). In contrast, the mean Spring Intermonsoon surface chlorophyll *a* value of 0.15 mg Chl m^{-3} was typical of oligotrophic oceanic regions. During the Spring and Fall Intermonsoons there was no onshore/offshore gradient in productivity or chlorophyll *a* from S02 to S11 (Figs. 9 and 10, Table 2).

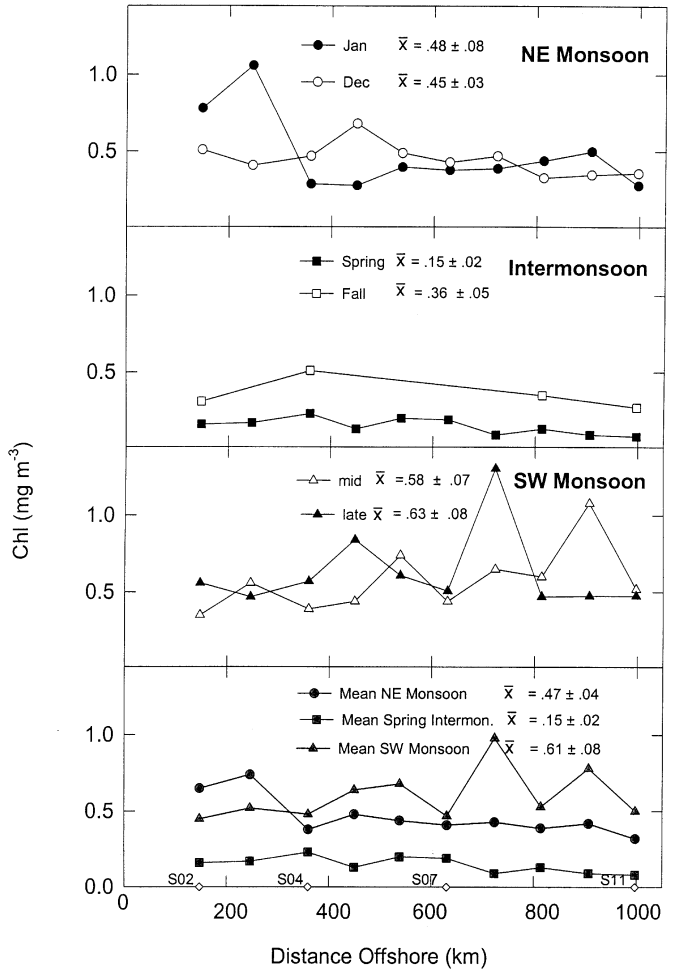

Fig. 10. Surface chlorophyll *a* along the southern section from S02 to S11. The Fall Intermonsoon chlorophyll (TN053, Table 1) is shown but not included in the mean in the bottom panel because only a few stations were occupied on the southern section during that cruise.

The January 1995 NE Monsoon period was more productive than the December 1995 NE Monsoon period (137 versus 88 mmol $C\,m^{-2}\,d^{-1}$) (Table 2) and productivity maxima in January 1995 were midway along the section at about 450 km and 800 km offshore (Fig. 9). In contrast, mean surface chlorophyll *a* concentrations during the two NE Monsoon periods were similar (0.48 versus 0.45 mg Chl *a* m^{-3}) (Fig. 10, Table 2). The highest surface chlorophyll *a* value (1.06 mg Chl *a* m^{-3}) during the January period was about 250 km offshore; as in all other seasons, there was no onshore/offshore gradient in productivity or chlorophyll *a*. The January 1995 NE Monsoon period had clear primary productivity maxima but no spatial gradient, while the December 1995 NE Monsoon had no clear maximum nor gradient. Minimal productivity values of about 85 mmol $C\,m^{-2}\,d^{-1}$ were the same in the two NE Monsoon periods and were essentially the same as the mean Intermonsoon productivity (80–86 mmol $C\,m^{-2}\,d^{-1}$) (Fig. 9).

Table 3
Maximum and minimum integrated primary productivity (mmol C $m^{-2}d^{-1}$), surface chlorophyll *a* (mg Chl m^{-3}) and P^B_{opt} (mmol C mg $Chl^{-1}d^{-1}$) values and, in parentheses, their location on the US-JGOFS southern section. P^B_{opt} is the highest water column productivity in a 24-h on-deck incubation normalized by chlorophyll concentration at the depth of the highest water column productivity

	NE Monsoon Jan	Intermonsoon spring	SW Monsoon		NE Monsoon Dec	Mean + SE
			Mid	Late		
Maximum values						
PP	202 (S09)	112 (S10)	184 (S10)	181 (S08)	121 (S06)	160 ± 18
Chl *a* (surf.)	1.06 (S03)	0.23 (S04)	1.08 (S10)	1.31 (S08)	0.68 (S05)	0.87 ± 0.19
P^B_{opt}	17.79 (S06)	20.81 (S10)	15.28 (S09)	17.18 (S11)	12.16 (S10)	16.64 ± 1.43
Minimum values						
PP	84 (S11)	65 (S05)	81 (S02)	70 (S09)	76 (S02)	75 ± 3
Chl *a* (surf.)	0.28 (S11)	0.08 (S11)	0.35 (S02)	0.47 (S03/S09)	0.33 (S09)	0.30 ± 0.06
P^B_{opt}	8.23 (S05)	6.14 (S06)	7.89 (S11)	7.00 (S03)	5.78 (S02)	7.01 ± 0.48

The SW Monsoon period was the most productive and had the highest values of surface chlorophyll *a*. Interestingly, two of the three highest productivity values of the SW Monsoon occurred at the same location (S08), about 700 km offshore in the region of assumed negative curl and Ekman downwelling (Table 2). These two productivity measurements were also very similar (183 versus 181 mmol $C\,m^{-2}\,d^{-1}$). Surface chlorophyll *a* had a maximum of 1.08 mg Chl *a* m^{-3} during the mid-SW Monsoon at Station S10, about 900 km from the coast, and 1.31 mg Chl *a* m^{-3} during late SW Monsoon at Station S08 (Fig. 10).

3.4. *Seasonal variability in* in situ *station profiles*

When profiles of biological properties are plotted for each of the five cruises that occupied the four long in situ stations along the southern section, a consistent pattern of seasonal variability emerges (Fig. 11).

At the inshore station, S02, productivity was highest during the January NE Monsoon; it decreased to one-fifth the January value during the Spring Intermonsoon. Productivity values at S02 during the two SW Monsoon cruises (mid and late) were very similar, about one-third the January NE Monsoon value. The December NE Monsoon had a productivity level intermediate between the SW Monsoon values and the relatively low Spring Intermonsoon productivity. Surface chlorophyll *a* had a ranking more or less parallel with that of productivity; that is, NE Monsoon chlorophyll *a* was highest and Spring Intermonsoon was lowest with a five-fold range; the other seasons fell between these two extremes. Chlorophyll *a*, unlike productivity, had a well-developed subsurface maximum in every season except the mid-SW Monsoon.

At Station S04, 359 km off the coast (Fig. 11), productivity was relatively low during the January NE Monsoon, but, as at Station S02, productivity in the upper three-fourths of the euphotic zone was lowest during the Spring Intermonsoon when Station S04 had the "typical tropical profile" (Longhurst, 1998) of a well-stratified, oligotrophic oceanic region. Highest productivity values at

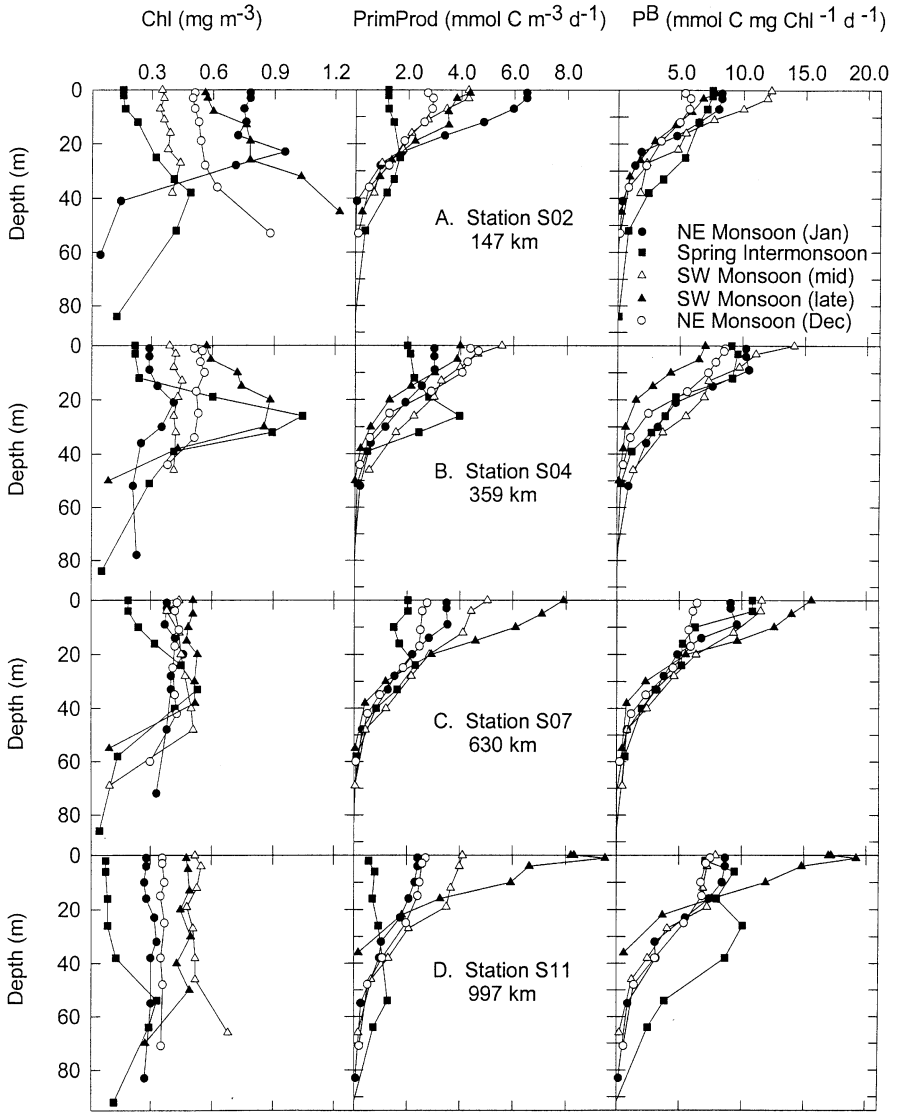

Fig. 11. Vertical profiles of chlorophyll *a*, primary productivity and chlorophyll-specific productivity (P^B) at S02, S04, S07 and S11 for five periods. P^B is the primary productivity at a given depth in the water column normalized by chlorophyll *a* concentration at that depth.

Station S04 occurred during the mid-SW Monsoon and the December NE Monsoon, with the next highest during the late SW Monsoon. The annual range of surface productivity at Station S04 was about one-third or one-half the range at Stations S02, S07 and S11.

At S07, 630 km offshore, productivity values (Fig. 11) had well-defined seasonal differences and fit the expected seasonal pattern. Late SW Monsoon was highest, followed in descending order by mid-SW Monsoon, January NE Monsoon, December NE Monsoon and Spring Intermonsoon,

which was the lowest, about one-fourth the late SW Monsoon level. The annual range of variability in surface chlorophyll *a* was extremely small, with all seasons except Spring Intermonsoon having between 0.35 and 0.55 mg m^{-3}. Spring Intermonsoon chlorophyll *a* values were lowest, but, as at Station S04, there was a subsurface maximum at about 35 m.

At Station S11, about 1000 km offshore (Fig. 11), the seasonal pattern was similar to that of Station S07, with highest productivity during the late SW Monsoon and lowest during the Spring Intermonsoon. Variation in productivity at Station S11 was large, with a ten-fold difference between the highest values (late SW Monsoon) and the lowest (Spring Intermonsoon). Furthermore, the seasonal maximum and minimum were higher and lower than at any other in situ station. During 1995 Station S11, about 1000 km offshore, was more variable in terms of productivity than any other in situ station on the southern section.

During the seasonal cycle, observations of biomass-normalized photosynthetic performance (P^B_{opt}) cluster between 8 and 12 mmol C mg Chl a^{-1} d^{-1} (Fig. 11). The lowest P^B_{opt} values in 1995 were during the December NE Monsoon at Stations S02, S07 and S11, with the annual minimum value (6 mmol C mg Chl a^{-1}) at S02. The highest P^B_{opt} values in the 1995 in situ station profiles were at the inshore stations, S02 and S04, during the mid-SW Monsoon and at the offshore stations, S07 and S11, during the late SW Monsoon (Fig. 11). As with primary productivity, P^B_{opt} values for the entire year were highest at Station S11, approaching 20 mmol C mg Chl a^{-1}. Surface chlorophyll *a* values varied four-fold at S02, two-fold at S04, two-fold at S07 and five-fold at S11. The inshore (S02, 147 km) and offshore (S11, 997 km) stations of the southern section were the most variable in chlorophyll *a*. At all four stations the lowest surface chlorophyll *a* concentrations were during the Spring Intermonsoon.

3.5. Filament at S08

Acoustic Doppler current profiler (Flagg and Kim, 1998) and satellite (Manghnani et al., 1998) observations revealed the presence of a strong, narrow current filament at Station S08 during the late SW Monsoon. Also at Station S08, an intermediate length station 723 km offshore, there were peaks in integrated primary productivity (Fig. 9, Table 2), surface chlorophyll *a* (Fig. 10, Table 2) and maximal water-column productivity, P_{opt} (Fig. 2). Surface productivity (Fig. 12) at Station S08 was about twice that of Station S07 and about four times that of Station S09.

Vertical profiles for Stations S07, S08 and S09 characterize the filament in terms of its vertical profile of properties (Fig. 12). These graphs indicate that Stations S07 and S09, the stations just inshore and offshore of the filament, were essentially identical in the upper 50 m in temperature, salinity, nitrate and chlorophyll *a* properties, while Station S08, which was close to the center of the filament, was distinct from its nearest neighbors in these properties. Temperature and, more significantly, salinity at Station S08 were lower than at both Station S07 and Station S09. Furthermore, the salinity values in the upper 50 m at Stations S07 and S09 are identical. The lower salinity surface water of the filament at Station S08 was underlain with higher salinity water at 60–80 m. Nitrate in the filament ($\approx 6\,\mu M$) was twice the concentration of that in the adjacent stations ($\approx 3\,\mu M$). Silicic acid in the filament was not elevated in parallel with nitrate. Station S07 had ML silicic acid values of $\approx 1.5\,\mu M$, Station S08 had $\approx 2\,\mu M$ and Station S09 had $\approx 3\,\mu M$. Relative to the nitrate concentration, silicic acid in Station S08 was significantly depleted.

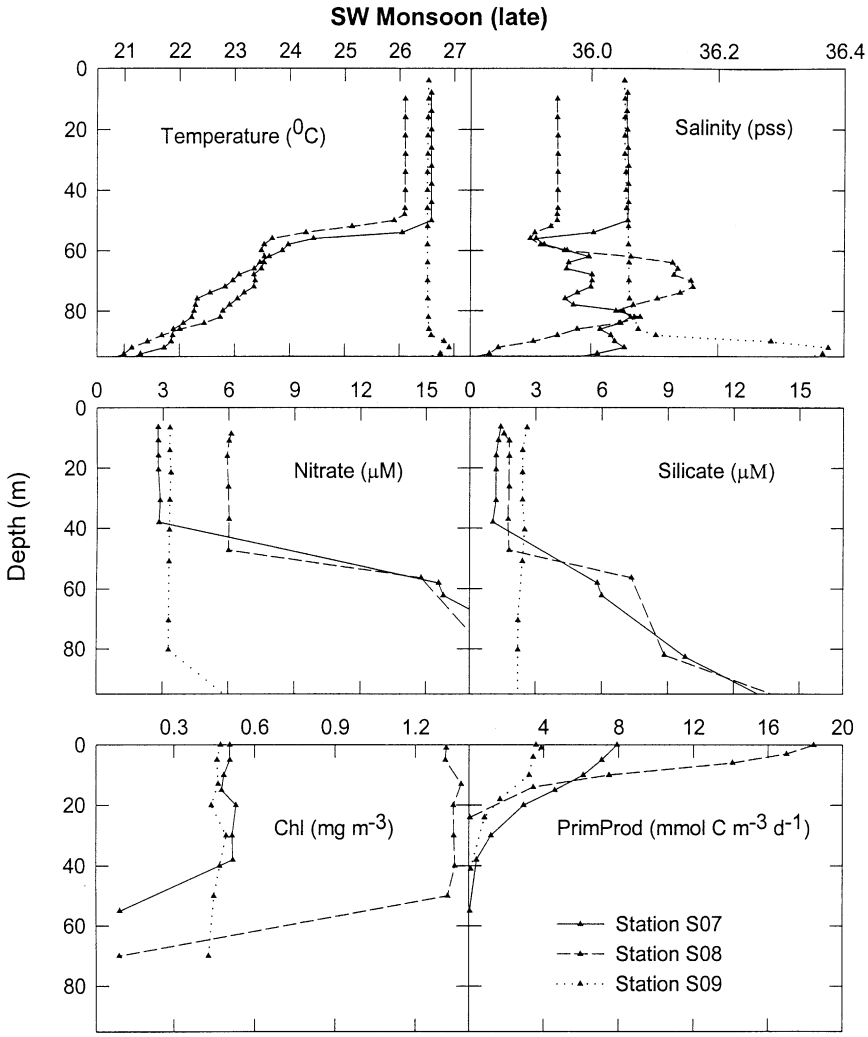

Fig. 12. Physical, chemical and biological properties at S07, S08 and S09 during the late SW Monsoon cruise (TN050). Satellite images and ADCP records indicate that S08 was in a strong jet-like current filament (Fig. 6 of Flagg and Kim, 1998).

4. Discussion

4.1. Comparison with other expeditions

While there is no systematic database of primary productivity for the region of the US JGOFS southern section, data are available from two expeditions, ANTON BRUUN in 1963 (Ryther et al., 1966) and Arabesque in 1994 (Savidge and Gilpin, 1999), that measured primary productivity along similar sections during the late SW Monsoon period (August–October). Cruise tracks for these

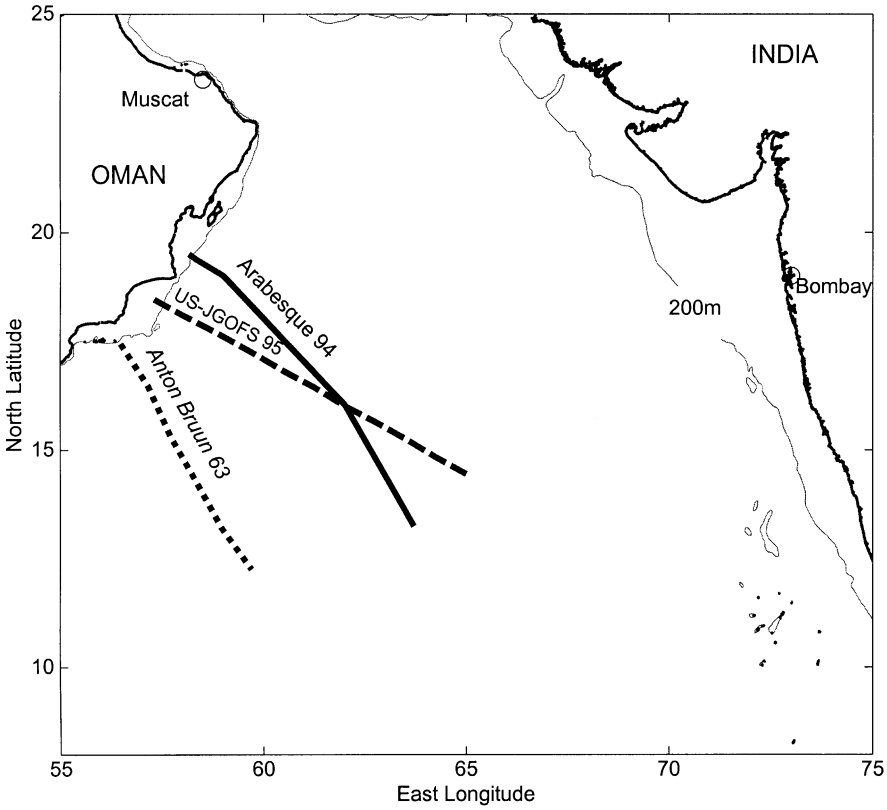

Fig. 13. A map showing the location of the Arabesque 1994 section (Savidge and Gilpin, 1999) and the ANTON BRUUN section in 1963 (Ryther et al., 1966) in relation to the US JGOFS southern section.

expeditions are shown in Fig. 13. Both expeditions made high-quality primary productivity determinations using trace metal clean techniques. The 1963 ANTON BRUUN expedition was carried out before there was awareness of the trace metal/primary production problem (Fitzwater et al., 1982; Sanderson et al., 1995); however, on the ANTON BRUUN cruise a Teflon™ and Pyrex™ sampler was attached at the end of the metallic hydrowire to collect water for primary productivity and dissolved organic carbon samples. Furthermore, when collecting water for the vertical profile that characterized the euphotic zone, a separate cast was made to each light depth. Apparently, this combination of a terminally attached Teflon™ and Pyrex™ sampler and separate casts greatly reduced trace-metal contamination from both the sampler and the hydrowire (Ryther and Menzel, 1965; Ryther et al., 1966; D. Menzel, personal communication).

Mean primary productivity observed by ANTON BRUUN in this region in 1963 (115 mmol C $m^{-2}d^{-1}$) was similar to US JGOFS observations in the same region (123 mmol C m^{-2} d^{-1}) as shown in Fig. 14. Also similar were the primary productivity values determined by Savidge and Gilpin (1999) in the same region on the Arabesque expedition (Burkill, 1999) during the 1994 SW Monsoon (127 mmol C m^{-2} d^{-1}) (Fig. 14). This comparison indicates that, as with meteorological observations, 1995 primary productivity, at least during the SW Monsoon, was similar in

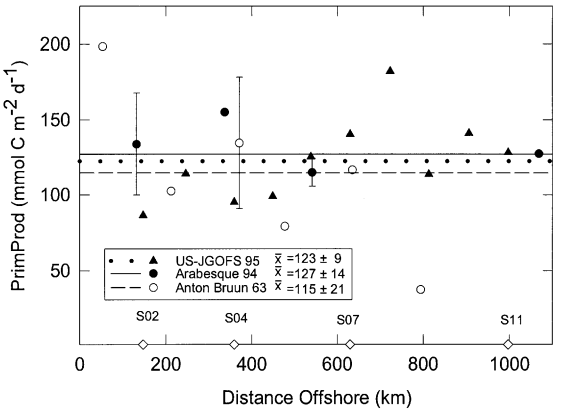

Fig. 14. A plot of integrated primary productivity versus distance offshore for the ANTON BRUUN 1963, Arabesque 1994, and US JGOFS 1995 cruises along the sections shown in Fig. 13. The symbols show values at each station along the sections; the horizontal lines show the mean primary productivity for each of the three expedition sections.

magnitude and pattern to previous years for which there are comparable primary productivity observations.

Qasim (1982) synthesized primary productivity and chlorophyll observations from 21 cruises that worked in the Arabian Sea between 1959 and 1976, including the International Indian Ocean Expedition (IIOE) results compiled by Krey and Babenerd (1976). Annual mean primary productivity for the Arabian Sea presented by Qasim (1982) was about 70 mmol C m^{-2} d^{-1}, which is considerably lower than the mean annual value for the southern section in 1995, 111 $\pm$ 11 mmol C m^{-2} d^{-1} (Table 2). However, a preponderance of the stations averaged by Qasim (1982) were located in the oligotrophic waters of the central and eastern Arabian Sea, i.e., east of 65°E. The areas designated by Qasim (1982) as "Coastal Waters" provide a better spatial comparison with the US JGOFS southern section. In coastal waters, Qasim (1982) reported a mean annual productivity of 110 mmol C m^{-2} d^{-1}. Considering that these 1959–1976 productivity observations were collected before Fitzwater et al. (1982) alerted the community to the need for trace-metal-clean procedures, this synthesis of early observations was surprisingly similar to the mean annual value obtained in this region in 1995 (111 $\pm$ 11 mmol C m^{-2} d^{-1}).

4.2. SW Monsoon primary productivity

High rates of primary productivity during the SW Monsoon have been well documented for many years (Ryther and Menzel, 1965; Ryther et al., 1966; Kabanova, 1968; Cushing, 1973; Krey, 1973; Zeitzschel, 1973; Krey and Babenerd, 1976; Qasim, 1977). However, before the US JGOFS study there were no time-series of primary productivity based on observations. Longhurst (1995 and 1998) presented a theoretical estimate of a SW Monsoon time-series of primary productivity with a maximum value during August of 280 mmol C m^{-2} d^{-1} and a mean value for the July–September period of 171 mmol C m^{-2} d^{-1}. In 1995, the observed SW Monsoon maximum productivity was about 180 mmol C m^{-2} d^{-1} (Table 3) and the mean was 123 mmol C m^{-2} d^{-1} (Fig. 9), both values being considerably lower than Longhurst's (1998). During 1995,

values as high as 280 mmol C m^{-2} d^{-1} were observed, but only in shallow water on the continental shelf close to the Omani coast (data available at http://www1.whoi.edu/jgofs.html.). Arabesque and earlier expeditions also observed values in that range ($>$ 280 mmol m^{-2} d^{-1}) on the shelf (Ryther et al., 1966; Owens et al., 1993; Savidge and Gilpin, 1999).

In September/October 1986, Owens et al. (1993) observed productivity of 116 mmol C m^{-2} d^{-1} in the vicinity of the mid-southern section. In August 1987, Bauer et al. (1991) and Olson et al. (1993) observed a mean of 86 $\pm$ 4 mmol C m^{-2} d^{-1} at three stations in the vicinity of the offshore end of the southern section. A large number of early Soviet observations synthesized by Kabanova (1968) gave a SW Monsoon mean of 91 mmol C m^{-2} d^{-1} for the region of the southern section. Cushing (1973) reanalyzed the Soviet data on a finer spatial scale, showing a mean of 121 mmol C m^{-2} d^{-1} for the region equivalent to the inner half of the southern section and 104 mmol C m^{-2} d^{-1} for the outer portion of the section. These mean SW Monsoon primary productivity values, ranging from 86 to 121 mmol C m^{-2} d^{-1}, are not very dissimilar from the mean SW Monsoon value obtained during 1995 (123 mmol C m^{-2} d^{-1}) (Fig. 9).

4.2.1. Spatial domain

An impressive feature of the biological response to the SW Monsoon observed in 1995 was the large offshore extent of the region with enhanced primary productivity. This observation was foreshadowed by Smith (1984), who speculated that "we have no way of knowing the exact areal extent of the biological response of the northwestern Indian Ocean including both Somali coastal waters and the Arabian Sea, but it is likely to exceed all other known areas of coastal upwelling." Why do the SW Monsoon winds enrich primary productivity over such a large area? There are several processes that might account for the large spatial extent: (1) so-called curl of the wind stress "offshore" upwelling, (2) offshore advection of nutrient-rich water by current filaments, (3) wind-driven mixing and (4) eddy-driven upwelling. Convective mixing, another process that enriches a large area in the central Arabian Sea, occurs only in boreal winter during the NE Monsoon when evaporative cooling dominates the heat flux.

Smith and Bottero (1977) first proposed that offshore upwelling occurs in the Arabian Sea, and Smith (1995) described how the process works in this particular upwelling system: a gradient (or "curl") in the alongshore wind causes an Ekman divergence (or convergence) with associated upwelling (or downwelling) at the bottom of the Ekman layer. The seaward increase in wind stress that characterizes coastal upwelling regions produces a gradient (positive wind-stress curl) that extends the upwelling influence farther offshore. However, Smith (1995) estimated that this positive curl enhances coastal upwelling by only a few percent in the world's four major eastern boundary current upwelling regions (Barber and Smith, 1981) because the offshore gradient of increased wind stress is relatively weak. In contrast, the Arabian Sea, during the SW Monsoon, is characterized by a very strong offshore wind maximum with a strong wind-stress gradient. During the 1995 SW Monsoon the wind jet crossed the southern section between S06 and S07 (Fig. 1) (Weller et al., 1998), so a positive gradient ("curl") was present from the coast out to about 600 km.

Smith and Bottero (1977) and Smith (1995) estimated that offshore Ekman upwelling extended about 200 km offshore and upwelled a volume of water of about the same magnitude as water upwelled by the coastal divergence. Fig. 5 shows that wind stress increased (i.e., the curl was positive) from Stations S04 to S07 during both the mid- and late SW Monsoon. According to the explanations of Smith (1995), the wind-stress gradient shown in Fig. 5 would force Ekman

upwelling farther offshore than the 200 km estimated by Smith and Bottero (1977). On the basis of wind stress observed in 1995, significant offshore Ekman upwelling (W_{EK}) took place at Station S07 and inshore at Station S02, but not at Station S04 (Fig. 7). The mid-SW Monsoon nitrate maxima at Stations S02 and S07 with a relative minimum at Station S04 (Fig. 6) independently support this interpretation of two spatially separate source regions separated by a non-upwelling region.

The results reported here indicate that the SW Monsoon significantly increases primary productivity over a large spatial domain that reaches from 150 to at least 1000 km offshore. The large area of positive wind-stress curl has been known for a long time (Hastenrath and Lamb, 1979) and its physical consequences have been estimated (Smith and Bottero, 1977), but these results specifically confirm the speculation of Smith (1984) that the biological response to the SW Monsoon takes place over at least half of the Arabian Sea basin.

4.2.2. Filaments and eddies

In 1995 the Arabian Sea in the vicinity of the southern section was dominated by eddies and filaments (Brink et al., 1996; Flagg and Kim, 1998; Lee et al., 2000). The presence of a strong advective filament at Station S08 during TN050 was shown by Flagg and Kim (1998, Fig. 6b), whose ADCP results indicate there was a strong, narrow, alongshore filament flowing northward in the upper 100 m at 508 km offshore; this narrow current was not present at Station S07 (630 km offshore) on TN050. Unfortunately, high winds and extreme sea-state conditions prevented collection of ADCP data from Stations S11 to S09. As mentioned previously, Station S10 during the late SW Monsoon cruise (TN050) was the only station of the entire Arabian Sea Expedition that was cancelled due to extreme sea state. However, observations of the same filament were obtained on TN051, a Sea Soar cruise of the ONR Forced Upper Ocean Dynamics project (Smith et al., 1998a), which profiled the Station S07 to S09 region about 3 weeks after the late SW Monsoon cruise (TN050). Flagg and Kim (1998) show that 3 weeks after the productivity work, the axis of the current had precessed inshore to Station S07 and was absent from Station S09.

During the sequence from early August (TN049), through early September (TN050) to the end of September (TN051), the strong jet-like current filament first precessed offshore. Reaching its maximum offshore extent during the late SW Monsoon cruise (TN050), the filament then moved inshore slightly where ONR SeaSoar cruise TN051 profiled it (Flagg and Kim, 1998). During early (TN053) and late (TN054) December 1995, the offshore filament was completely absent from Station S08 and the southern section. The north- flowing filament also was absent from Station S08 and its environs a year earlier in late December 1994 and January 1995 during NE Monsoon cruise TN043 (Flagg and Kim, 1998). Taken together, the ADCP observations show that the offshore "S08 filament" was present continuously, crossing in the outer southern section, from about mid-July to mid-October.

Information on the biological character of filaments, given in Fig. 4 of Latasa and Bidigare (1998), shows depth distribution of chlorophyll *a* at Station S08 and the adjacent stations. The chlorophyll *a* maximum is vertically uniform at about 1.30 mg Chl *a* m^{-3} from the surface to 60 m. Fig. 5 of Latasa and Bidigare (1998) shows the presence of a strong fucoxanthin maximum at Station S08, indicating that Station S08 was dominated by diatoms. Cluster analysis (Latasa and Bidigare, 1998) shows that Station S08 pigment properties cluster with Station N01, an inshore station on the northern section where there was intense local upwelling during the late SW Monsoon period (TN050).

Nitrate was about 6 μM in the filament compared to 3 μM at Stations S07 and S09 (Fig. 12), but silicic acid, unlike other inorganic plant nutrients, was depleted in the filament. Uptake of silicic acid by the abundant diatoms in the filament, which were documented by Latasa and Bidigare (1998), would account for the atomic ratio deficiency of Si relative to N. The Si:N ratio at Station S08 was a low 0.25 during the late SW Monsoon cruise (TN050). Chlorophyll *a* in the ML of the filament was three times the concentration in the adjacent stations, while surface productivity in the filament was two times higher than at Station S07 and four times higher than at Station S09.

The dramatic biological richness discontinuity of the filament at Station S08 is demonstrated by the presence of the highest biomass and primary productivity observed during the late SW Monsoon period (Table 2, Figs. 9 and 10). P^{B}_{opt} in the filament was 14.72 mmol C mg Chl a^{-1} d^{-1} (Table 2), a value considerably higher than those observed during EqPac (Barber et al., 1996), NABE (Chipman et al., 1993) or the Southern Ocean (Smith et al., in press). Clearly, the filament supported both high specific rates and high biomass accumulation.

The Arabian Sea filaments are dynamically distinct from the well-studied filaments of the California Current off northern California and Oregon (Chavez et al., 1991). The California Current filaments do not extend nearly as far offshore as the Arabian Sea filaments, but Brink et al. (1998) point out that when the length of the filament is scaled by the square root of the Coriolis parameter (due to the difference in latitude) the filaments are similar in length. Despite the similarity when scaled, filaments in the coastal transition zone off northern California are distinct because they did not have a maximum in nutrient or phytoplankton concentration within the dynamic feature (Chavez et al., 1991). With surface waters in their high-speed core having relatively low concentrations and strong cross-jet gradients of nutrients and biomass, the California filaments were dynamic boundaries separating nutrient-rich inshore coastally upwelled water from offshore oligotrophic water. Fig. 8 of Chavez et al. (1991) is parallel to Fig. 12 of this report: both figures plot profiles from the filament and just inshore and offshore of it. Comparison of the two figures shows nitrate and biomass maxima in the Arabian Sea filament, while in the California Current filament concentrations are intermediate between the inshore maximum and offshore minimum.

Frequent ADCP profiling during the US JGOFS Arabian Sea cruises together with analysis of hydrographic properties (Flagg and Kim, 1998) shows that these strong, narrow currents transport inshore water to the central Arabian Sea. While the current filament was present and well defined 723 km offshore, at least a portion of the water in this filament was upwelled adjacent to the Omani coast, as indicated by the physical and chemical properties of water in the filament (Arnone et al., 1996; Brink et al., 1996, 1998; Manghnani et al., 1998). The lower temperature of the filament indicates that the water was recently upwelled, but the low salinity in the upper 50 m and the slightly higher salinity at depth indicate that the cool, surface water of the filament was not locally upwelled (Fig. 12).

It is clear that Arabian Sea filaments advect a significant amount of water rich in nutrients and phytoplankton offshore about 700 km. We speculate that nutrients provided by filaments (and eddies) in the Arabian Sea contribute as much to the increased areal extent of the highly productive region as does offshore upwelling, a suggestion made earlier on the basis of modeling by Young and Kindle (1994) and Keen et al. (1997). Along with increasing the area of high productivity, the filaments also provide the specific physical, chemical and biological conditions required for the accumulation of moderately high diatom biomass (Latasa and Bidigare, 1998). This accumulation

of diatom biomass sets the stage for high export rates. Honjo et al. (1999) suggest that the Arabian Sea filaments are involved in or even primarily responsible for the high rates of offshore carbon export that characterize the region during the SW Monsoon (Nair et al., 1989; Buesseler et al., 1998; Lee et al., 1998). The primary productivity observations reported here from filaments support the suggestion of Honjo et al. (1999).

In addition to the presence of filaments, the Arabian Sea region also was characterized by the presence of numerous mesoscale eddies (Flagg and Kim, 1998). These eddies may play as large a role as filaments in the nutrient budget of the offshore region; McGillicuddy and Robinson (1997) have established that such eddies can significantly enrich surface waters. Future Arabian Sea work will have to resolve eddy, as well as filament, dynamics. Achieving a predictive understanding of the role of the Arabian Sea in global cycles will require investigation of the role played by filaments and eddies in increasing primary productivity, structuring the composition of the pelagic phytoplankton community, and regulating carbon export to deep waters.

4.2.3. Downwelling and deep mixing

The brief May 1995 downwelling pulse at Station S07 (Fig. 7) is the only evidence for the often hypothesized and modeled Ekman downwelling that is assumed to occur along the southern section in the offshore negative-curl region (Fig. 1) (Luther, 1987; Bauer et al., 1991, 1992; Bartolacci and Luther, 1999). Unfortunately, no process cruises occupied the southern section during May, so the US JGOFS team of chemical and biological investigators did not sample this downwelling pulse. The observed large-scale pattern of Ekman upwelling and downwelling during the 1995 SW Monsoon differed somewhat from the pattern that is hypothesized, on the basis of models, to characterize this region (Brock et al., 1991). Large-scale, but weak, Ekman downwelling occupied a large region (about half the area of the northern Arabian Sea in the western Arabian Sea), but it was most intense south of 10°N and east of 60°E (Halpern et al., 1998; Lee et al., 2000).

Ekman downwelling intense enough to force light or nutrient limitation was simply never found at any of the 1995 stations along the US JGOFS southern section. The SW Monsoon maxima for primary productivity, chlorophyll *a* and P^{B}_{opt} were located at Stations S08, S09, S10 and S11 (Table 3), offshore of the mean position of the Findlater Jet. Furthermore, high rates of P^{B}_{opt} (ranging from 7.89 to 17.18 mmol C mg Chl a^{-1} d^{-1}) (Table 2) indicate no reduction of photosynthetic performance by light or nutrient limitation. Taken together, these results convincingly confirm that there was no reduction of primary productivity, biomass or photosynthetic performance in the putative negative curl region. The high vertical flux rates in this region (Lee et al., 1998) were not forced by decreased photosynthetic performance that caused phytoplankton to lose the ability to regulate buoyancy (Waite et al., 1992).

A parallel argument can be made regarding wind-driven mixing during the SW Monsoon. Mixed-layer depths along the southern section deepen offshore (Fig. 5), increasing from 10 to 15 m at Station S02 to a maximum of about 75 m at Station S11. Surprisingly, the ML nitrate concentrations decrease over the offshore gradient where the ML deepens. Wind-driven mixing during both SW Monsoon periods was simply not deep enough to erode the nutricline and allow replacement of nutrients taken up by the vigorous productivity on the offshore half of the southern section, Stations S07–S11 during the SW Monsoon. Similarly, the high productivity, biomass and specific rates at these stations indicate that the wind-driven mixing was not deep enough to have any detectable deleterious effect on photosynthetic activity.

4.3. Primary productivity during the non-SW Monsoon period

The comparison of 1995 primary productivity values with earlier observations is extremely interesting for the remaining (non-SW Monsoon) periods of the year because the US JGOFS observations differ markedly from earlier observations. Longhurst's (1998) conceptual model estimates that productivity during the rest of the year is relatively constant at about 60 mmol $C\,m^{-2}\,d^{-1}$ through the Spring and Fall Intermonsoons and the NE Monsoon. In agreement with Longhurst (1998), Radhakrishna et al. (1978), Nair and Pillai (1983) and Jochem et al. (1993) report mean values around 60 mmol C m^{-2} d^{-1} for the NE Monsoon and Intermonsoon periods; and, while 60 mmol C $m^{-2}\,d^{-1}$ is low compared to SW Monsoon primary productivity values, it is high relative to other areas of the tropical and temperate ocean (Barber et al., 1996; Karl et al., 1996). For example, the tropical Pacific Ocean in 1992 had mean values of 29 mmol C $m^{-2}\,d^{-1}$ north and south of the equatorial zone, and even the enriched equatorial Pacific zone of 10°N – 10°S had a mean of only 52 ± 7 mmol $C\,m^{-2}\,d^{-1}$ (Barber et al., 1996). Thus Longhurst's (1998) 60 mmol C m^{-2} d^{-1} prediction is a relatively high level of productivity for an offshore region that was considered to be oligotrophic for the non-SW Monsoon period of the year (Smith, 1991).

The estimate of 60 mmol C m^{-2} d^{-1} is considerably lower than the lowest seasonal values observed in 1995, which were 86 mmol C m^{-2} d^{-1} during the Spring Intermonsoon and 80 mmol C m^{-2} d^{-1} during the Fall Intermonsoon (Fig. 9). The minimum primary productivity values observed in each season in 1995 varied from 65 to 84 mmol C m^{-2} d^{-1} with a mean minimum of 75 mmol C m^{-2} d^{-1} (Table 3), which is considerably higher than the non-SW Monsoon value of 60 mmol C m^{-2} d^{-1} (Radhakrishna et al., 1978; Jochem et al., 1993) or the even lower mean value of about 40 mmol C m^{-2} d^{-1} (Olson et al., 1993; Owens et al., 1993). The relatively large difference in non-SW Monsoon primary productivity between our 1995 values and those in the literature may result in part from sampling different offshore regions, with most of the earlier literature values coming from along or east of 65°E and the 1995 observations coming mostly from west of 65°E. The higher winds observed in the 1995 Spring Intermonsoon period relative to the typically low climatological mean Intermonsoon winds may have been another factor involved in the unexpectedly high 1995 primary productivity. Understanding the source of this disagreement remains an important Arabian Sea issue.

4.3.1. NE Monsoon primary productivity

The NE Monsoon period was a period of steady and moderate winds, clear skies, low humidity and strong heat transfer from the ocean to the atmosphere (Weller et al., 1998). Meteorological observations from 1994 and 1995 show that the cool, dry winds blowing out of central Asia during the NE Monsoon extracted heat (and water) from the surface layer in December 1994 and January 1995 (Prasanna Kumar and Prasad, 1996; Weller et al., 1998). During the NE Monsoon evaporative cooling both decreased the ML temperature and increased ML salinity, producing dense water that convectively mixed (Weller et al., 1998). The only portion not undergoing convective mixing during the NE Monsoon was the coastal region adjacent to the coast of Oman (Morrison et al., 1998).

Morrison et al. (1998) show that the offshore half of the southern section had surface salinity >36 pss during the January NE Monsoon cruise (TN043). Cooling of this high salinity surface water forced convective mixing deep enough to erode into the nutricline. The cooler and slightly

more saline surface water convectively mixed down to 90 or 100 m over the offshore half of the southern section (Fig. 5) in January 1995. Because the nutricline is typically at 80 to 90 m (Conkright et al., 1994), this mixing entrained nutrients into the surface ML and produced ML nitrate concentrations of 3–5 μM (Fig. 6). Offshore convective mixing during the NE Monsoon was first suggested by Banse (1984) as a source of nutrients to support enhanced winter productivity rates such as those observed in the January 1995 NE Monsoon period when surface heat loss was taking place. Banse and McClain (1986) proposed that there is significant interannual variability of winter convective mixing; small differences in the surface heat exchange could enhance convective mixing in one year and shut it off in another. Fig. 9 shows that the 1994/1995 winter NE Monsoon (January) had two productivity maxima of about 200 mmol C m^{-2} d^{-1}, while the 1995/1996 Winter NE Monsoon (December) had no maxima and the mean productivity, 88 mmol C m^{-2} d^{-1}, was about the same as that during the Spring Intermonsoon, 86 mmol C m^{-2} d^{-1}. This variation in the primary productivity in the NE Monsoons of two consecutive years may result because, in the December 1995 NE Monsoon, not enough cooling had taken place to force the convective mixing that characterized the January 1995 NE Monsoon.

Madhupratap et al. (1996) were the first to show the connection between convective mixing, nutrient enrichment and productivity enhancement in the Arabian Sea. Their observations are mostly from a section on 64°E from 10°N–21°N. This central Arabian Sea region is generally much less productive than the western half of the basin (Longhurst, 1998), so it is not surprising that their NE Monsoon values from the north–south section are lower than those observed by the US JGOFS Arabian Sea Study in the same year on the southern section in the western half of the basin. In Madhupratap et al. (1996), the maximum NE Monsoon value observed on the 64°E section was 50 mmol C m^{-2} d^{-1}, about twice the maximum Spring Intermonsoon value (28 mmol C m^{-2} d^{-1}). Similarly, along the southern section in 1995 the maximum NE Monsoon rate observed on the US JGOFS cruise (202 mmol C m^{-2} d^{-1}) was about twice the maximum Spring Intermonsoon value (112 mmol C m^{-2} d^{-1}). While the central Arabian Sea is less productive than the western Arabian Sea in the region of the southern section, the proportional NE Monsoon productivity enhancement relative to Intermonsoon productivity was about the same in both regions. The observations of Madhupratap et al. (1996) together with the US JGOFS observations reported here show that a large spatial domain of the Arabian Sea is enriched by convective mixing.

During both the January and December NE Monsoons the deepest ML depths along the southern section were offshore at Stations S07 and S11 (Fig. 5). Neither primary productivity nor P^{B}_{opt} at these offshore stations was reduced by this 80–90 m mixing. During the January NE Monsoon, Station S09, in the center of the deep convective mixing region, had the highest primary productivity value observed along the southern section during the entire year (Tables 2 and 3, Fig. 9). The value, 202 mmol C m^{-2} d^{-1}, was considerably higher than the mean SW Monsoon value of 123 mmol C m^{-2} d^{-1}. The productivity values at adjacent stations where there were deep MLs (Fig. 5) in both the January and December NE Monsoons did not have productivity values that were reduced relative to those on the inshore half of the section where MLs were much shallower (Table 2, Fig. 9). In addition, specific growth rates were close to maximal values and were twice those of the Spring Intermonsoon (Caron and Dennett, 1999). Clearly, there was no Sverdrup (1953) critical depth limitation of productivity caused by deep convective mixing during either of the NE Monsoon periods in 1995; the second hypothesis was not supported.

4.3.2. Intermonsoons

During the Spring and Fall Intermonsoon periods the MLs were very shallow and nutrient concentrations were low over the entire study area (Figs. 5 and 6). The Intermonsoon periods in the Arabian Sea are customarily referred to as oligotrophic periods, but their productivity values of 86 ± 5 mmol C m^{-2} d^{-1} (Spring) and 80 ± 12 mmol C m^{-2} d^{-1} (Fall) (Fig. 9) are two to three times the off-equator productivity in the tropical Pacific Ocean (29 ± 2 mmol C m^{-2} d^{-1}) (Barber et al., 1996) or the multi-annual mean at the central North Pacific HOT site (39 mmol C m^{-2} d^{-1}) (Karl et al., 1995) (Table 4).

Nitrate and other new nutrients (*sensu* Dugdale and Goering, 1967) were close to detection limits along the entire southern section during the Spring Intermonsoon and only slightly higher during

Table 4
Primary productivity in four regions where the JGOFS protocols were used to determine productivity. Values expressed are the mean ± S.E. Values for the Arabian Sea are from the US JGOFS southern section only (Fig. 1)

Region	Primary productivity (mmol C m^{-2} d^{-1})	Reference
Arabian Sea (1995)		
NE Monsoon (Jan)	137 ± 13	This report
Spring Intermonsoon	86 ± 5	This report
SW Monsoon (mid)	135 ± 10	This report
SW Monsoon (late)	110 ± 10	This report
NE Monsoon (Dec)	88 ± 4	This report
Annual Mean	111 ± 11	
Equatorial Pacific at 140°W (1992)		
1°N to 1°S	95 ± 6	Barber et al., (1996)
2°N to 2°S	86 ± 4	Barber et al., (1996)
5°N to 5°S	74 ± 7	Barber et al., (1996)
10°N to 10°S	52 ± 7	Barber et al., (1996)
> 10°N and > 10°S	29 ± 2	Barber et al., (1996)
North Atlantic at 47°N (1989)		
Spring bloom (April/May)	107 ± 23	Chipman et al., (1993)
Spring bloom (late May)	90 ± 4	Martin et al., (1993)
Mean spring bloom	99	
Central North Pacific at 24°N		
HOT non-ENSO period	32 ± 8	Karl et al., (1995)
HOT ENSO period	45 ± 9	Karl et al., (1995)
Multi-annual mean	39	
Ross Sea (Antarctica)		
Spring Bloom (Nov)	95 ± 9	Smith et al., (in press)
Summer Post Bloom (Jan/Feb)	49 ± 5	Smith et al., (in press)
Antarctic Polar Frontal Zone		
Pre Bloom (Nov)	33 ± 6	Hiscock et al., (submitted)
Spring Bloom (Dec)	69 ± 6	Hiscock et al., (submitted)
Post Bloom (Feb/Mar)	20 ± 2	Hiscock et al., (submitted)

the Fall Intermonsoon (Fig. 6). Vertical profiles of chlorophyll *a* and primary productivity are lowest during the Spring Intermonsoon (Fig. 11), showing the consequences of no upwelling (Fig. 7), shallow mixed layers (Fig. 5), and low nutrient concentrations (Fig. 6). However, the strong stratification during this period produces subsurface maxima in chlorophyll *a* and productivity along the entire section. In subsurface maxima at Station S04, chlorophyll *a* concentrations reached about 1.0 mg m^{-3} and productivity reached 4 mmol C m^{-3} d^{-1}. Eddy diffusion of new nutrients across the steep Intermonsoon nutricline (Morrison et al., 1998) along with recycling of regenerated nutrients provided nutrients adequate to develop the strong Intermonsoon subsurface maxima (McCarthy et al., 1999).

The annual time-series of properties at Station S07 (Fig. 8) shows the association during the Intermonsoons of shallow MLs, no Ekman upwelling, nitrate well below the K_s concentration and low primary productivity. Iron decreases only slightly during the Intermonsoon periods (Fig. 8) and its concentration remains many times higher than the observed iron K_s value (Coale et al., 1996a). During the Spring Intermonsoon, P^B_{opt} values differ from the low biomass and primary productivity values in that P^B_{opt} values are about equal to other periods in the Arabian Sea (Table 2, Fig. 11) and high relative to other oceanic regions (Barber et al., 1996; Smith et al., in press). The Spring Intermonsoon in 1995 was a period of minimal phytoplankton abundance and primary productivity, but also a period of efficient photosynthetic performance. The phytoplankton there, although in low concentrations, were in good photophysiological health and were photosynthesizing at high specific rates of productivity relative to those in other ocean regions (Marra et al., 2000). At the same time, their specific growth rates were lower than all of the other periods in 1995 (Landry et al., 1998; Brown et al., 1999; Caron and Dennett, 1999).

4.4. *Chlorophyll* a *variability*

In contrast to primary productivity, there are several seasonal analyses of chlorophyll from ship and satellite observations (Banse, 1987; Yoder et al., 1993; Banse and English, 1994, 2000; Longhurst, 1998). Banse (1987) and Banse and English (2000) treat the various subregions as defined by Colborn (1975) on the basis of seasonal thermal structure. The Banse and English (2000) Box 3A includes the southern section from about Station S04 to Station S08, and Box 3B approximately covers the region from Station S09 to Station S11; their Table 1 presents monthly mean values for each year. Unfortunately, because of cloud cover, no images from the July/August period are available in this comprehensive reanalysis, so Banse and English (2000) used the September images as surrogates for the SW Monsoon period. Satellite observations for Box 3A show September values from 0.39–2.57 mg Chl m^{-3} in the 1978–1986 period. Farther offshore, in Box 3B, the September values ranged from 0.42–1.70 mg Chl m^{-3}. In comparison, during the two SW Monsoon cruises in 1995 we observed values of 0.39–1.31 mg Chl *a* m^{-3} for the Box 3A stations and values of 0.47–1.08 mg Chl *a* m^{-3} for the Box 3B stations (Table 2).

The 1995 US JGOFS Arabian Sea process cruises did not work in the region in April or May when Banse and English (2000) record minimal values (ranging for Box 3A from 0.05–0.16 mg Chl m^{-3}; for Box 3B, from 0.07–0.13 mg Chl m^{-3}). For the Spring Intermonsoon, therefore, it is necessary to compare values for March, the period covered by the process cruise. Banse and English (2000) report March values for Box 3A of 0.16–0.34 mg Chl m^{-3} and for Box 3B, 0.17–0.32 mg Chl m^{-3}. The March cruise recorded values for Stations S04 to S08 (Box 3A) of

0.09–0.23 mg Chl *a* m^{-3} and for Stations S09 to S10 (Box 3B) values of 0.08–0.13 mg Chl *a* m^{-3} (Table 2). In Banse and English (2000), the NE Monsoon (January) values in Box 3A ranged from 0.15 to 0.65 mg Chl m^{-3} and in Box 3B, 0.22–0.64 mg Chl m^{-3} during the 9 years of CZCS observation. The 1995 NE Monsoon cruise values in the Box 3A stations ranged from 0.29 to 0.38 mg Chl *a* m^{-3} and in the Box 3B stations, 0.28–0.5 mg Chl *a* m^{-3} (Table 2).

As expected, the range of values during the 9 years of CZCS observations is wider than the range of the 1995 observations, but, in general, there is agreement between the equivalent periods. This agreement gives considerable confidence that the shipboard and satellite time-series of phytoplankton pigments in the offshore regions are comparable, but it also serves to emphasize the need for rigorous reprocessing such as that done by Banse and English (2000).

While there is remarkably good agreement on the magnitude of seasonal variability in the offshore region, the consensus concept also holds that there are strong spatial chlorophyll gradients during the SW Monsoon period with elevated inshore concentrations. The composite (1978–1986) CZCS images, such as in Longhurst (1998, Color Plates 1–4) or the seasonal images on the NASA Earth Observing System (EOS) website, *http://daac.gsfc.nasa.gov/CAMPAIGN.DOCS/OCDST/classic_scenes/04_classics_arabian.html*, show strong gradients. The representative seasonal images are, of course, composites and therefore not equivalent to observations from any single cruise. Despite this difficulty, we note that in 1995 there were no observations of high inshore values or a spatial gradient in chlorophyll consistent with the CZCS composite image for the SW Monsoon period.

Using CZCS observations, Brock and McClain (1992) analyzed spatial variability during the SW Monsoon in three zones of vertical motion: inshore coastal upwelling, positive-curl offshore upwelling and negative-curl downwelling. They estimated that water upwelled in the coastal domain extended to about 150 km offshore. Within this coastal upwelling domain, their CZCS images record relatively high pigment concentrations of > 5.0 mg m^{-3}. It is interesting that Banse and English (2000), using more stringent reprocessing criteria, also report values from 1.50–5.53 mg Chl m^{-3} in the inshore region (Box 1A) during September. Our Station S02 is in the Omani Shelf coastal upwelling as delimited by Brock and McClain (1992), yet no chlorophyll *a* values approaching 5.0 mg Chl m^{-3} were observed there in 1995 (Fig. 6, Table 2). Low temperature (Fig. 5) and high nitrate values (15 μM) (Fig. 6) observed at Station S02 show the presence of recently upwelled water. Furthermore, wind-stress calculations (Fig. 7) indicate that Station S02 was the site of relatively strong Ekman upwelling (about 1.4 m d^{-1}) during the SW Monsoon. Considering the well-defined upwelling that was enriching Station S02 when the ship sampled there, it remains puzzling why repeated sampling has never observed the high chlorophyll concentrations (> 5 mg Chl m^{-3}) shown in CZCS observations. The absence of onshore/offshore gradients and very high inshore chlorophyll concentrations is a characteristic of the Arabian Sea about which shipboard observations disagree not only with the consensus concept, but with theory and models (Luther, 1987; Bauer et al., 1991; Brock et al., 1991; McCreary et al., 1996) as well as satellite climatology (Longhurst, 1998) and NASA website images.

4.5. Regulation of photosynthetic performance

The SW and NE Monsoons were periods when new nutrients were at or above the half-saturation concentration for uptake (Fig. 8) (McCarthy et al., 1999). The 1°N–1°S equatorial wave

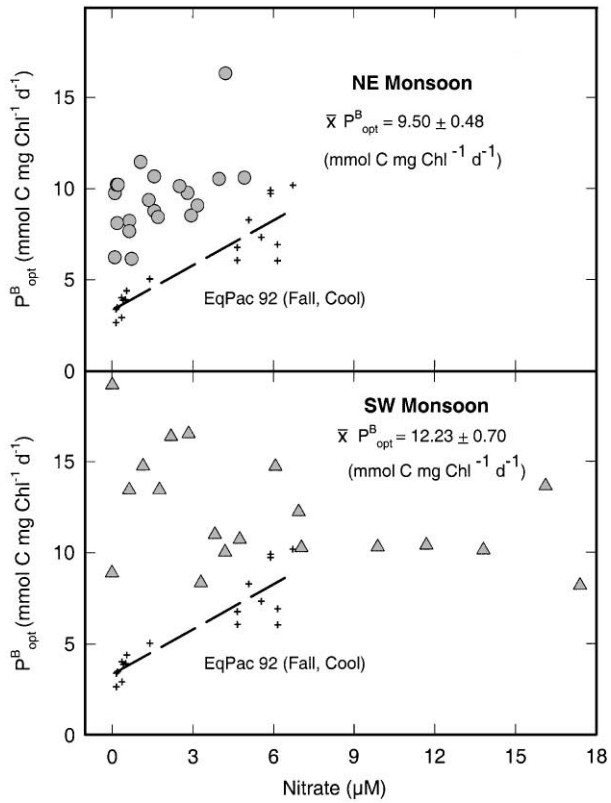

Fig. 15. P^{B}_{opt}, the highest water column productivity in a 24-h on-deck incubation normalized by chlorophyll *a* concentration at the depth of the highest water column productivity, as a function of nitrate concentration in the NE and SW Monsoon seasons. The dashed line and small crosses show the P^{B}_{opt} versus nitrate relationship from the equatorial Pacific Ocean HNLC region during Fall 1992 when cool, high-nutrient ENSO conditions were present on the equator (Barber et al., 1996).

guide in the equatorial Pacific Ocean also had abundant macronutrients during the 1992 US JGOFS EqPac study (Barber et al., 1996), yet P^{B}_{opt} was significantly lower than in the Arabian Sea (Fig. 15). During the 1995 SW Monsoon the lowest P^{B}_{opt} value, about 7 mmol C mg Chl a^{-1} d^{-1}, was close to the maximum equatorial Pacific Ocean value, about 8 mmol C mg Chl a^{-1} d^{-1}. Given that macronutrient concentrations as well as light (E_0) and temperature in the two regions are similar, the enhanced photosynthetic performance in the Arabian Sea must result from increased availability of a limiting micronutrient; clearly, iron is the best candidate for the micronutrient limiting photosynthetic performance (P^{B}_{opt}) (Lindley et al., 1995; Lindley and Barber, 1998).

The source of iron in the Arabian Sea is iron-rich dust supplied by the SW Monsoon blowing off Africa (Husar et al., 1997; Measures and Vink, 1999; Tindale and Pease, 1999). Fig. 15 provides evidence that the iron source (atmospheric fallout) was uncoupled from the macronutrient source (upwelling and mixing). If the micronutrient iron and the macronutrients were provided from the same subsurface source, as they are in the equatorial Pacific Ocean, the P^{B}_{opt} versus nitrate relationship would have a positive slope. During the SW Monsoon the P^{B}_{opt} versus

nitrate relationship had no slope and during the NE Monsoon there was only a very weak suggestion of a positive slope.

From the high P^B_{opt} values at very low nitrate values (Fig. 15), we also can infer that when iron was abundant, recycled nitrogen, such as ammonia and urea (McCarthy et al., 1999), were sufficient for maintaining the high photosynthetic performance we observed. Note also that the mean P^B_{opt} of 10.68 ± 0.65 (Table 2) for all stations for the entire year was higher than the mean 1992 value for the 1°N–1°S equatorial wave guide (about 8 mmol C mg Chl^{-1} d^{-1}) (Barber et al., 1996), suggesting that the monsoonal eolian subsidies keep the Arabian Sea iron-enriched (relative to the equatorial Pacific Ocean) throughout the year. Witter et al. (2000) found total ligand concentration in the Arabian Sea was higher than concentrations in the western North Atlantic or Pacific Oceans. This rich ligand background would keep iron delivered by dust deposition soluble in seawater for extended intervals.

Two consequences of micronutrient replete conditions are that fundamental photosynthetic properties, such as quantum yield, are determined solely by photoadaption and the magnitude of these properties is in the range of values indicative of nutrient sufficient growth (Marra et al., 2000).

The 1995 Arabian Sea study was, in effect, a natural iron addition experiment that complemented the IronEx experiments carried out in the iron-poor equatorial Pacific HNLC waters in 1993 and 1995 (Martin et al. 1994; Coale et al., 1996b). That the highest specific productivity rates (P^B_{opt}) were observed during the SW Monsoon when iron input and iron concentrations were highest is consistent with the suggestion that iron availability directly regulates photosynthetic performance when macronutrients are replete (Lindley et al., 1995; Lindley and Barber, 1998).

4.6. Regulation of primary productivity

Arabian Sea primary productivity has three salient characteristics:

1. Throughout the year and over a large spatial domain, it is high relative to other oceanic regions and the mean annual value roughly equals maximum productivity values in other nutrient-rich, offshore oceanic regions (Table 4),
2. While high, it is lower than expected during the intense SW Monsoon upwelling, given the high nutrients, micronutrients, and incident irradiance (E_0) as well as the absence of wind mixing or downwelling deep enough to limit photosynthetic performance (P^B_{opt}), and
3. During the non-SW Monsoon portion of the year, especially during the Intermonsoon periods, primary productivity is higher than expected, given the absence of any obvious physical mechanism to supply nutrients to the euphotic zone.

The first characteristic is a consequence of physical and chemical conditions that support enhanced rates of photosynthetic performance (P^B_{opt}), which in turn support moderately high primary productivity. For example, the 1995 mean mid-SW Monsoon Arabian Sea productivity, averaged along the entire 1000 km southern section, (135 mmol C m^{-2} d^{-1}) exceeded the 1992 productivity maximum (95 mmol C m^{-2} d^{-1}) in the 1°N–1°S equatorial wave guide at 140°W in the Pacific Ocean and the 1989 mean North Atlantic spring bloom productivity (99 C m^{-2} d^{-1}) (Table 4).

Given high P^B_{opt} rates, the reason primary productivity is less than expected during intense upwelling is that biomass (chlorophyll) does not accumulate to very high levels. There is, of course,

no puzzle about how the pico- and nanophytoplankton are held to low concentrations despite high specific growth rates. Efficient grazing by protozoan zooplankton keep growth and loss in "balance" as defined by Landry et al. (1997). The growth rate of micrograzers and, hence, the grazing rate were coupled to the growth rate of the small phytoplankton during all seasons in the Arabian Sea (Landry et al.,1998; Brown et al., 1999; Caron and Dennett, 1999). Growth rates were accompanied by grazing losses that prevented the accumulation of significant biomass (Smith et al., 1998b; Landry et al., 1998; Brown et al., 1999; Roman et al., 2000) except in a few special hydrographic situations, such as in filaments (Fig. 12) or eddies (Bidigare et al., 1997).

The puzzle is, given the favorable nutrient, micronutrient, irradiance (E_0), N:Si ratio and rapid onset of SW Monsoon upwelling, why didn't a diatom bloom of 5–10 mg Chl *a* m^{-3} develop, as happens in the Peruvian upwelling (Barber and Smith, 1981)? The convincing explanation given by Smith et al. (1998b) is that the large-bodied copepod *Calanoides carinatus* is present in large numbers in the upwelling waters after having "over wintered" in deep water during the period between SW Monsoons. The abundance of these hungry copepods in the initially upwelled water means that there is no reproductive lag in zooplankton abundance and, therefore, maximal grazing pressure is present as diatom specific growth rates begin to increase during onset of the SW Monsoon upwelling. The unique life cycle of *Calanoides carinatus* keeps the diatom/copepod gain and loss terms balanced just as the pico- and nanophytoplankton/micrograzer gain and loss terms are balanced.

5. Conclusions

(a) In 1995 along a 1000-km section from the Omani coast to the central Arabian Sea, the SW Monsoon had the highest productivity (123 ± 9 mmol C m^{-2} d^{-1}) and this productivity was high relative to other oceanic regions; the NE Monsoon productivity (112 ± 7 mmol C m^{-2} d^{-1}) was nearly as high.

(b) Productivity during the Spring Intermonsoon (86 ± 6 mmol C m^{-2} d^{-1}) was much higher than oligotrophic regions such as the tropical Pacific Ocean (29 ± 2 mmol C m^{-2} d^{-1}) or the North Pacific gyre region (32 ± 8 mmol C m^{-2} d^{-1}).

(c) The annual mean productivity (111 ± 11 mmol C m^{-2} d^{-1}) in 1995 along this section from the Omani coast to the central Arabian Sea was about equal to the spring bloom maximum (107 ± 23 mmol C m^{-2} d^{-1}) during the 1989 North Atlantic Bloom Experiment (NABE) and the equatorial, 1°N–1°S wave guide maximum (95 ± 6 mmol C m^{-2} d^{-1}) in the Pacific Ocean during the 1992 EqPac study.

(d) There was little or no onshore/offshore gradient in primary productivity from 150 to 1000 km off the Omani coast; there was, however, considerable mesoscale spatial variability along the 1000-km section in 1995.

(e) The SW Monsoon primary productivity observed in 1995 (123 ± 9 mmol C m^{-2} d^{-1}) was very similar to that observed in the same region in 1994 by the Arabesque Expedition (127 ± 14 mmol C m^{-2} d^{-1}) and in 1964 by the ANTON BRUUN Expedition (115 ± 27 mmol C m^{-2} d^{-1}).

(f) During the SW Monsoon, coastal upwelling, offshore upwelling, wind-driven mixing, advection in filaments and eddy upwelling provided new nutrients to a broad region of the Arabian Sea that reached about 800 km off the Omani coast.

(g) During the NE Monsoon, convective mixing was the major physical process providing new nutrients to a widespread region of the Arabian Sea.
(h) Energetic filaments extending offshore to about 700 km supported growth and accumulation of diatoms which resulted in high productivity and biomass maxima.
(i) No evidence of light limitation of either primary productivity or photosynthetic performance (P^{B}_{opt}) from deep convective mixing during the NE Monsoon, deep wind mixing during the SW Monsoon or offshore Ekman downwelling during the SW Monsoon was observed at any location in 1995.
(j) High rates of photosynthetic performance ($P^{B}_{opt} > 10$ mmol C mg Chl a^{-1} d^{-1}) relative to other oceanic regions indicate that the Arabian Sea during the SW Monsoon was more iron replete than the equatorial Pacific Ocean.
(k) Dissolved iron concentrations well above observed iron K_s concentrations and high iron ligand concentrations kept iron recycling and accounted for the year-round high values of photosynthetic performance (P^{B}_{opt}).
(l) As hypothesized, the SW Monsoon was the most productive period, but the mean SW Monsoon primary productivity values were lower than expected because grazing by copepods overwintering in the upwelled water kept diatoms from accumulating the biomass (> 5 mg Chl a m^{-3}) characteristic of upwelling regions with high levels of primary productivity.

Acknowledgements

Major support for this research was provided by the Harvey W. Smith Endowment at Duke University with ancillary support from the National Science Foundation as part of the US JGOFS Arabian Sea Process Study. We especially thank the crew of the University of Washington's able ship, R/V THOMAS G. THOMPSON. We also thank members of the primary productivity team who are not co-authors: Elaine Barber, Lisa Borden, Fei Chai, Anna Hilting, Mike Hiscock, Carol Knudson and Steve Lindley. The research by DH was performed at the Jet Propulsion Laboratory, California Institute of Technology, under contract with the National Aeronautics and Space Administration. This is US JGOFS Contribution 507.

References

Arnone, R.L., Macintosh, P., Kindle, J., Brink, K.H., Lee, C., 1996. Filaments structures along the Oman coast during the Monsoon. EOS, Transactions, American Geophysical Union 77 (46), F382.

Aruga, Y., 1973. Primary Production in the Indian Ocean II. In: Zeitschel, B. (Ed.), The Biology of the Indian Ocean. Springer, New York, pp. 127–130.

Banse, K., 1984. Overview of the hydrography and associated biological phenomena in the Arabian Sea, off Pakistan. In: Haq, B.U., Milliman, J.D. (Eds.), Marine Geology and Oceanography of Arabian Sea and Coastal Pakistan. Von Nostrand Reinhold, New York, pp. 271–303.

Banse, K., 1987. Seasonality of phytoplankton chlorophyll in the central and northern Arabian Sea. Deep-Sea Research I 34, 713–723.

Banse, K., English, D.C., 1994. Seasonality of coastal zone color scanner phytoplankton pigment in the offshore oceans. Journal of Geophysical Research 99, 7323–7345.

Banse, K., English, D.C., 2000. Geographical differences in seasonality of CZCS-derived phytoplankton pigment in the Arabian Sea for 1978–1986. Deep-Sea Research II 47, 1623–1677.

Banse, K., McClain, C.R., 1986. Winter blooms of phytoplankton in the Arabian Sea as observed by the coastal zone color scanner. Marine Ecology Progress Series 34, 201–211.

Barber, R.T., Borden, L., Johnson, Z., Marra, J., Knudson, C., Trees, C., 1997. Ground truthing modeled k_{par} and on deck primary productivity incubations with in situ observations. Society of Photo-Optical Instrumentation Engineers 2963, 834–839.

Barber, R.T., Sanderson, M.P., S.T. Lindley, F.C., Newton, J., Trees, C.C., Foley, D.G., Chavez, F. P., 1996. Primary productivity and its regulation in the equatorial Pacific during and following the 1991-92 El Niño. Deep-Sea Research II 43, 933–969.

Barber, R.T., Smith, R.L., 1981. Coastal upwelling ecosystems. In: Longhurst, A. (Ed.), Analysis of Marine Ecosystems. Academic Press, New York, pp. 31–68.

Bartolacci, D.M., Luther, M.E., 1999. Patterns of co-variability between physical and biological parameters in the Arabian Sea. Deep-Sea Research II 46, 1933–1964.

Bauer, S., Hitchcock, G.L., Olson, D.B., 1991. Influence of monsoonally-forced Ekman dynamics upon surface layer depth and plankton biomass distributions in the Arabian Sea. Deep-Sea Research I 38, 531–553.

Bauer, S., Hitchcock, G.L., Olson, D.B., 1992. Arabian Sea surface layer depth and biomass distribution as influenced by Ekman dynamics. In: Desai, B.N. (Ed.), Proceedings of the International Symposium on the Oceanography of the Indian Ocean. Oxford & IBH Publishing Co Pvt Ltd., New Delhi, pp. 583–593.

Behrenfeld, M.J., Falkowski P, .G., 1997. Photosynthetic rates derived from satellite-based chlorophyll concentration. Limnology and Oceanography 42, 1–20.

Bender, M., Orchardo, J., Dickson, M.-L., Barber, R.T., Lindley, S., 1999. In vitro O_2 fluxes compared with ^{14}C production and other rate terms during the JGOFS Equatorial Pacific experiment. Deep-Sea Research I 46, 637–654.

Bender, M.L., Grande, K., Johnson, K., Marra, J., Williams, P., Sieburth, J., Pilson, M., Langdon, C., Hitchcock, G., Orchardo, J., Hunt, C., Donaghay, P., Heinemann, K., 1987. A comparison of four methods for the determination of planktonic community metabolism. Limnology and Oceanography 32, 1085–1098.

Bertrand, P., Lallier-Vergès, E., 1993. Past sedimentary organic matter accumulation and degradation controlled by productivity. Nature 364, 786–788.

Bidigare, R.R., Latasa, M., Johnson, Z., Barber, R.T., Trees, C.C., Balch, W.M., 1997. Observations of a *Synechococcus*-dominated cyclonic eddy in open-oceanic waters of the Arabian Sea. Ocean Optics XIII 2963, 260–265.

Brink, K.H., Arnone, R., Coble, P., Flagg, C., Jones, B., Kindle, J., Lee, C., Phinney, D., Wood, M., Yentsch, C., Young, D., 1998. Monsoons boost biological productivity in Arabian Sea. EOS, Transactions, American Geophysical Union 79, 168–169.

Brink, K.H., Jones, B.H., Lee, C.M., Wood, M., 1996. A cool filament off Oman, June 1995; origins and fates of its water. EOS, Transactions, American Geophysical Union 77 (46), F382.

Brock, J.C., McClain, C.R., 1992. Interannual variability in phytoplankton blooms observed in the northwestern Arabian Sea during the Southwest Monsoon. Journal of Geophysical Research 97, 733–750.

Brock, J.C., McClain, C.R., Hay, W.W., 1992. A southwest monsoon hydrographic climatology for the Northwestern Arabian. Journal of Geophysical Research 97, 9455–9465.

Brock, J.C., McClain, C.R., Luther, M.E., Hay, W.W., 1991. The phytoplankton bloom in the northwestern Arabian Sea during the southwest monsoon of 1979. Journal of Geophysical Research 96, 20 623–20 642.

Brown, S.L., Landry, M.R., Barber, R.T., Campbell, L., Garrison, D.L., Gowing, M.M., 1999. Picophytoplankton dynamics and production in the Arabian Sea during the 1995 Southwest Monsoon. Deep-Sea Research II 46, 1745–1768.

Buesseler, K., Ball, L., Andrews, J., Benitez-Nelson, C., Belastock, R., Chai, F., Chao, Y., 1998. Upper ocean export of particulate organic carbon in the Arabian Sea derived from thorium-234. Deep-Sea Research II 42, 2461–2488.

Burkill, P.H., 1999. ARABESQUE: An overview. Deep-Sea Research II 46, 529–547.

Caron, D.A., Dennett, M.R., 1999. Phytoplankton growth and mortality during the 1995 Northeast Monsoon and Spring Intermonsoon in the Arabian Sea. Deep-Sea Research II 46, 1665–1690.

Chavez, F.P., Barber, R.T., Kosro, P.M., Huyer, A., Ramp, S., Stanton, T., de Mendiola, B.R., 1991. Horizontal transport and the distribution of nutrients in the coastal transition zone off northern California: effects on primary production, phytoplankton biomass and species composition. Journal of Geophysical Research 96, 14 833–14 848.

Chipman, D.W., Marra, J., Takahashi, T., 1993. Primary production at 47 degrees N and 20 degrees W in the North Atlantic Ocean: A comparison between the carbon-14 incubation method and the mixed layer carbon budget. Deep-Sea Research II 40, 151–169.

Coale, K.H., Fitzwater, S.E., Gordon, R.M., Johnson, K.S., Barber, R.T., 1996a. Control of community growth and export production by upwelled iron in the equatorial Pacific Ocean. Nature 379, 621–624.

Coale, K.H., Johnson, K.S., Fitzwater, S.E., Gordon, R.M., Tanner, S., Chavez, F.P., Ferioli, L., Sakamoto, C., Rogers, P., Millero, F., Steinberg, P., Nightingale, P., Copper, D., Cochlan, W.P., Kudela, R., 1996b. A massive phytoplankton bloom induced by an ecosystem-scale iron fertilization experiment in the equatorial Pacific Ocean. Nature 383, 495–501.

Colborn, J.G., 1975. The Thermal Structure of the Indian Ocean. University Press of Hawaii, Honolulu, 173pp.

Conkright, M.E., Levitus, S., Boyer, T.P., Bartolacci, D.M., Luther, M.E., 1994. Atlas of the Northern Indian Ocean. University of South Florida, St. Petersburg, FL, 150pp.

Currie, R.I., Fisher, A.E., Hargreaves, P.M., 1973. Arabian Sea Upwelling. In: Zeitschel, B. (Ed.), The Biology of the Indian Ocean. Springer, New York, pp. 37–52.

Cushing, D.H., 1973. Production in the Indian Ocean and the Transfer from the Primary to the Secondary Level. In: Zeitschel, B. (Ed.), The Biology of the Indian Ocean. Springer, New York, pp. 475–486.

Dickson, M.-L., Orchardo, J., Barber, R.T., Marra, J., McCarthy, J.J., Sambrotto, R.N., 2001. Production and respiration rates in the Arabian Sea during the 1995 Northeast and Southwest Monsoons. Deep-Sea Research II 48, 1199–1230.

Dietrich, G., 1973. The Unique Situation in the Environment of the Indian Ocean. In: Zeitzschel, B. (Ed.), The Biology of the Indian Ocean. Springer, New York, pp. 1–6.

Dugdale, R.C., Goering, J.J., 1967. Uptake of new and regenerated forms of nitrogen in primary production. Limnology and Oceanography 12, 196–206.

Fieux, M., Stommel, H., 1977. Onset of the Southwest Monsoon over the Arabian Sea from marine reports of surface winds. Monthly Weather Review 105, 231–236.

Findlater, J., 1971. Mean monthly air flow at low levels over the western Indian ocean. Geophysical Memoirs 115, 53 pp. Her Majesty's Stationery Office, Norwich, England, UK.

Fitzwater, S., Knauer, G.A., Martin, J.H., 1982. Metal contamination and its effect on primary production measurements. Limnology and Oceanography 27, 544–551.

Flagg, C.N., Kim, H.-S., 1998. Upper ocean currents in the northern Arabian Sea from shipboard ADCP measurements collected during 1994–1996 the US JGOFS and ONR programs. Deep-Sea Research II 45, 1905–1915.

Gardener, W.D., Gundersen, J.S., Richardson, M.J., Walsh, I.D., 1999. The role of seasonal and diel changes in mixed-layer depth on carbon and chlorophyll distributions in the Arabian Sea. Deep-Sea Research II 46, 1833–1858.

Garrison, D.L., Gowing, M.M., Hughes, M.P., 1998. Nano- and microplankton in the northern Arabian Sea during the Southwest Monsoon August–September, 1995: a U.S. JGOFS study. Deep-Sea Research II 45, 2269–2299.

Goericke, R., Repeta, D., 1993. Chlorophyll *a* and *b* and divinyl chlorophylls *a* and *b* in the open sub-tropical North Atlantic Ocean. Marine Ecology Progress Series 101, 307–313.

Gross, F., Zeuthen, E., 1948. The buoyancy of plankton diatoms: a problem of cell physiology. Proceedings of the Royal Society B 135, 382.

Halpern, D., Freilich, M.H., Weller, R.A., 1998. Arabian Sea surface winds and ocean transports determined from ERS-1 scatterometer. Journal of Geophysical Research – Oceans 103, 7799–7806.

Halpern, D., Woiceshyn, P.M., 1999. Onset of the Somali Jet in the Arabian Sea during June 1997. Journal of Geophysical Research – Oceans 104, 18 041–18 046.

Halpern, D., Woiceshyn, P.M., 2001. Somali Jet in the Arabian Sea, El Niño and India rainfall. Journal of Climate, in press.

Hansell, D.A., Carlson, C.A., 1998. Net community production of dissolved organic carbon. Global Biogeochemical Cycles 12, 443–453.

Hastenrath, S., Lamb, P.J., 1979. Climatic Atlas of the Indian Ocean. University of Wisconsin Press, 19 pp. + 97 charts.

Hiscock, M.R., Marra, J., Smith, W.O., Barber, R.T. On deck ground truthing using optical properties and in situ replicates. Deep-Sea Research II, submitted for publication.

Holm-Hansen, O., Lorenzen, C., Holmes, R., Strickland, J., 1965. Fluorometric determination of chlorophyll. Journal du Conseil International pour l'Exploration de la Mer 30, 3–15.

Honjo, S., Dymond, J., Prell, W., Ittekkot, V., 1999. Monsoon-controlled export fluxes to the interior of the Arabian Sea; U.S. JGOFS 1994–1995 experiment. Deep-Sea Research II 46, 1859–1902.

Hunter, C.N., Gordon, R.M., Fitzwater, S.E., Coale, K.H., 1996. A rosette system for the collection of trace metal clean seawater. Limnology and Oceanography 41, 1367–1372.

Huntsman, S.A., Barber, R.T., 1977. Primary production off northwest Africa: the relationship to wind and nutrient conditions. Deep-Sea Research 24, 25–34.

Husar, R.B., Prospero, J.M., Stow, L.L., 1997. Characterization of tropospheric aerosols over the oceans with the NOAA advanced very high resolution radiometer optical thickness operational product. Journal of Geophysical Research 102, 16889–16909.

Iverson, R.L., 1990. Control of marine fish production. Limnology and Oceanography 35, 1593–1604.

Iverson, R.L., Bittaker, H.F., Myers, V.B., 1976. Loss of radiocarbon in direct use of Aquasol for liquid scintillation counting of solutions containing ^{14}C-$NaHCO_3$. Limnology and Oceanography 21, 756–758.

Jeffrey, S.W., 1974. Profiles of photosynthetic pigments in the ocean using thin-layer chromatography. Marine Biology 26, 101–110.

Jochem, F.J., Pollehne, F., Zeitschel, B., 1993. Productivity regime and phytoplankton size structure in the Arabian Sea. Deep-Sea Research II 40, 711–735.

Kabanova, Y.G., 1968. Primary production of the northern part of the Indian Ocean. Oceanology 8, 214–225.

Karl, D.M., Christian, J.R., Dore, J.E., Hebel, D.V., Letelier, R.M., Tupas, L.M., Winn, C.D., 1996. Seasonal and interannual variability in primary production and particle flux at Station ALOHA. Deep-Sea Research I 43, 539–568.

Karl, D.M., Letelier, R., Hebel, D., Tupas, L., Dore, J., Christian, J., Winn, C., 1995. Ecosystem changes in the North Pacific subtropical gyre attributed to the 1991–1992 El Niño. Nature 373, 230–234.

Karl, D.M., Winn, D.D., Hebel, D.V., Letelier, R., 1990. Hawaii Ocean Time series program: field and laboratory protocols. University of Hawaii, 187pp.

Keen, T.R., Kindle, J.C., Young, D.K., 1997. The interaction of southwest monsoon upwelling, advection and primary production in the northwest Arabian Sea. Journal of Marine Systems 13, 61–82.

Krey, J., 1973. Primary Production in the Indian Ocean I. In: Zeitschel, B. (Ed.), The Biology of the Indian Ocean. Springer, New York, pp. 115–126.

Krey, J., Babenerd, B., 1976. Phytoplankton production. In: Atlas of the International Indian Ocean Expedition. Universitat Kiel, Institut fur Meereskunde, pp. 70 .

Landry, M.R., Barber, R.T., Bidigare, R.R., Chai, F., Coale, K.H., Dam, H.G., Lewis, M.R., Lindley, S.T., McCarthy, J.J., Roman, M.R., Stoecker, D.K., Verity, P.G., White, J.R., 1997. Iron and grazing constraints on primary production in the central equatorial Pacific: an EqPac synthesis. Limnology and Oceanography 42, 405–418.

Landry, M.R., Brown, S.L., Campbell, L., Constantinou, J., Liu, H., 1998. Spatial patterns in phytoplankton growth and microzooplankton grazing in the Arabian Sea during monsoon forcing. Deep-Sea Research II 45, 2353–2368.

Latasa, M., Bidigare, R., 1998. A comparison of phytoplankton populations of the Arabian Sea during the Spring Intermonsoon and Southwest Monsoon of 1995 as described by HPLC-analyzed pigments. Deep-Sea Research II 45, 2133–2170.

Laws, E.A., 1991. Photosynthetic quotients, new production and net community production in the open ocean. Deep-Sea Research I 38, 143–167.

Laws, E.A., Landry, M.R., Barber, R.T., Campbell, L., Dickson, M.-L., Marra, J., 2000. Carbon cycling in primary production bottle incubations: inferences from grazing experiments and photosynthetic studies using ^{14}C and ^{18}O in the Arabian Sea. Deep-Sea Research II 47, 1339–1352.

Lee, C., Murray, D.W., Barber, R.T., Buesseler, K.O., Dymond, J., Hedges, J.I., Honjo, S., Manganini, S.J., Marra, J., Peterson, M.L., Prell, W.L., Wakeham, S.G., 1998. Particulate organic carbon fluxes: Results from the US JGOFS Arabian Sea Process Study. Deep-Sea Research II 45, 2489–2501.

Lee, C.M., Jones, B.H., Brink, K.H., Fischer, A.S., 2000. The upper-ocean response to monsoonal forcing in the Arabian Sea: seasonal and spatial variability. Deep-Sea Research II 47, 1177–1226.

Li, W.K.W., Maestrini, S.Y. (Eds.), 1993. Measurement of Primary Production from the Molecular to the Global Scale. ICES Marine Science Symposium, 286pp.

Lindley, S.T., Barber, R.T., 1998. Phytoplankton response to natural and artificial iron addition. Deep-Sea Research II 45, 1135–1150.

Lindley, S.T., Bidigare, R.R., Barber, R.T., 1995. Phytoplankton photosynthesis parameters along 140°W in the equatorial Pacific. Deep-Sea Research II 42, 441–463.

Lohrenz, S.E., Wiesenburg, D.A., Rein, C.R., Arnone, R.A., Taylor, C.D., Knauer, G.A., Knap, A.H., 1992. A comparison of *in situ* and simulated *in situ* methods for estimating oceanic primary production. Journal of Plankton Research 14, 201–221.

Longhurst, A., 1998. Ecological Geography of the Sea. Academic Press, 398pp.

Longhurst, A.R., 1993. Seasonal cooling and blooming in tropical oceans. Deep-Sea Research I 40, 2145–2165.

Longhurst, A.R., 1995. Seasonal cycles of pelagic production and consumption. Progress in Oceanography 36, 77–167.

Lorenzen, C.J., 1966. A method for continuous measurement of *in vivo* chlorophyll concentration. Deep-Sea Research 13, 223–227.

Luther, M.E., 1987. Indian Ocean modelling. In: Katz, E., Witte, J. (Eds.), Further Progress in Equatorial Oceanography. Nova University Press, Dania, FL, pp. 303–316.

Madhupratap, M., Prasanna Kumar, S., Bhattathiri, P.M.A., Kumar, M.D., Raghukumar, S., Nair, K.K.C., Ramaiah, N., 1996. Mechanism of the biological response to winter cooling in the northeastern Arabian Sea. Nature 384, 549–552.

Malone, T.C., Pike, S.E., Conley, D.J., 1993. Transient variations in phytoplankton productivity at the JGOFS Bermuda time series station. Deep-Sea Research I 40, 903–924.

Manghnani, V., Morrison, J.M., Hopkins, T.S., Bohm, E., 1998. Advection of upwelled waters in the form of plumes off Oman during the Southwest Monsoon. Deep-Sea Research II 45, 2027–2052.

Marra, J., Dickey, T.D., Ho, C., Kinkade, C.S., Sigurdson, D.E., Weller, R.A., Barber, R.T., 1998. Variability in primary production as observed from moored sensors in the central Arabian Sea in 1995. Deep-Sea Research II 45, 2253–2267.

Marra, J., Trees, C.C., Bidigare, R.R., Barber, R.T., 2000. Pigment absorption and quantum yields in the Arabian Sea. Deep-Sea Research II 47, 1279–1299.

Martin, J.H., et al., 1994. Testing the iron hypothesis in ecosystems of the equatorial Pacific Ocean. Nature 371, 123–129.

Martin, J.H., Fitzwater, S.E., Gordon, R.M., Hunter, C.N., Tanner, S.J., 1993. Iron, primary production and carbon-nitrogen flux studies during the JGOFS North Atlantic Bloom Experiment. Deep-Sea Research II 40, 115–134.

McCarthy, J.J., Garside, C., Nevins, J.L., 1999. Nitrogen dynamic during the Arabian Sea Northeast Monsoon. Deep-Sea Research II 46, 1623–1664.

McCreary Jr., J.P., Kohler, K.E., Hood, R.R., Olson, D.B., 1996. A four-component ecosystem model of biological activity in the Arabian Sea. Progress in Oceanography 37, 193–240.

McGill, D.A., 1973. Light and Nutrients in the Indian Ocean. In: Zeitschel, B. (Ed.), The Biology of the Indian Ocean. Springer, New York, pp. 53–102.

McGillicuddy, D.J., Robinson, A.R., 1997. Eddy-induced nutrient supply and new production in the Sargasso Sea. Deep-Sea Research I 44, 1427–1450.

Measures, C.I., Vink, S., 1999. Seasonal variations in the distribution of Fe and Al in the surface waters of the Arabian Sea. Deep-Sea Research II 46, 1597–1622.

Morrison, J.M., Codispoti, L.A., Gaurin, S., Jones, B., Manghnani, V., Zheng, Z., 1998. Seasonal variation of hydrographic and nutrient fields during the U.S. JGOFS Arabian Sea Process Study. Deep-Sea Research II 45, 2053–2101.

Nair, P.V.R., Pillai, V.K., 1983. Productivity of the Indian Seas. J. Mar. Biol. Assoc. India 25, 41–50.

Nair, R.V., Ittekkot, V., Manganini, S.J., Ramaswamy, V., Haake, B., Degens, E.T., Desai, B.N., Honjo, S., 1989. Increased particle flux to the deep ocean related to monsoons. Nature 338, 749–751.

Odum, E.P., 1971. Fundamentals of Ecology. Saunders, Philadelphia, 574pp.

Olson, D.B., Hitchcock, G.L., Fine, R.A., Warren, B.A., 1993. Maintenance of the low-oxygen layer in the central Arabian Sea. Deep-Sea Research II 40, 673–685.

Owens, N.J.P., Burkill, P.H., Mantoura, R.F.C., Woodward, E.M.S., Bellan, I.E., Aiken, J., Howland, R.J.M., Llewellyn, C.A., 1993. Size-fractionated primary production and nitrogen assimilation in the northwestern Indian Ocean. Deep-Sea Research II 40, 697–709.

Pace, M.L., Knauer, G.A., Karl, D.M., Martin, J.H., 1987. Primary production, new production and vertical flux in the eastern Pacific Ocean. Nature 325, 803–804.

Peterson, B.J., 1980. Aquatic primary productivity and the ^{14}C–CO_2 method: a history of the productivity problem. Annual Reviews of Ecology and Systematics 11, 359–385.

Prasanna Kumar, S., Prasad, T.G., 1996. Winter cooling in the northern Arabian Sea. Current Science 71, 834–841.

Qasim, S.Z., 1977. Biological productivity of the Indian Ocean. Indian Journal of Marine Sciences 6, 122–137.

Qasim, S.Z., 1982. Oceanography of the northern Arabian Sea. Deep-Sea Research 29, 1041–1068.

Radhakrishna, K., Devassy, V.P., Bhargava, R.M.S., Bhattathiri, P.M.A., 1978. Primary production in the Northern Arabian Sea. Indian Journal of Marine Sciences 7, 271–275.

Richardson, K., 1991. Comparison of ^{14}C primary production determinations made by different laboratories. Marine Ecology Progress Series 72, 189–201.

Robinson, C., Williams, P.J.leB., 1999. Plankton net community production and dark respiration in the Arabian Sea during September 1994. Deep-Sea Research II 46, 745–765.

Roman, M., Smith, S., Wishner, K., Zhang, X., Gowing, M., 2000. Mesozooplankton production and grazing in the Arabian Sea. Deep-Sea Research II 47, 1423–1450.

Ryther, J., Menzel, D.W., 1965. On the production, composition, and distribution of organic matter in the Western Arabian Sea. Deep-Sea Research 12, 199–209.

Ryther, J.H., Hall, J.R., Pease, A.K., Bakun, A., Jones, M.M., 1966. Primary production in relation to the chemistry and hydrography of the western Indian Ocean. Limnology and Oceanography 11, 371–380.

Sanderson, M.P., Hunter, C.N., Fitzwater, S.E., Gordon, R.M., Barber, R.T., 1995. Primary productivity and trace metal contamination measurements from a clean rosette system versus ultra clean Go-Flo bottles. Deep-Sea Research II 42, 431–440.

Sathyendranath, S., Stuart, V., Irwin, B.D., Maass, H., Savidge, G., Gilpin, L., Platt, T., 1999. Seasonal variations in bio-optical properties of phytoplankton in the Arabian Sea. Deep-Sea Research II 46, 633–653.

Savidge, G., Gilpin, L., 1999. Seasonal influences on size fractionated chlorophyll *a* concentrations and primary production in the north-west Indian Ocean. Deep-Sea Research II 46, 701–723.

SCOR, 1996. JGOFS Report No. 19: Protocols for the Joint Global Ocean Flux Study (JGOFS) Core Measurements. Scientific Committee on Oceanic Research, International Council of Scientific Unions, Bergen, 170pp.

Shi, W., Morrison, J.M., Böhm, E., Manghnani, V., 2000. The Oman upwelling zone during 1993 , 1994 and 1995. Deep-Sea Research II 47, 1227–1248.

Smayda, T.J., 1970. The suspension and sinking of phytoplankton in the sea. Oceanography and Marine Biology Annual Review 8, 353–414.

Smayda, T.J., Boleyn, B.J., 1965. Experimental observations on the flotation of marine diatoms. Limnology and Oceanography 10, 499–509.

Smetacek, V., 1980. Annual cycle of sedimentation in relation to plankton ecology in western Kiel Bight. Ophelia Supliment 1, 65–76.

Smetacek, V.H., Passow, U., 1990. Spring bloom initiation and Sverdrup's critical depth model. Limnology and Oceanography 35, 228–234.

Smith, R.L., 1995. The physical processes of coastal ocean upwelling systems. In: Summerhayes, C.P., Emeis, K.-C., Angel, M.V., Smith, R.L., Zeitschel, B. (Eds.), Upwelling in the Ocean: Modern Processes and Ancient Records. Wiley, Chichester, pp. 39–64.

Smith, R.L., Bottero, J.S., 1977. On upwelling in the Arabian Sea. In: Angel, M. (Ed.), A Voyage of Discovery. Pergamon Press, pp. 291–304.

Smith, S.L. (Ed.) 1991. U.S. JGOFS: Arabian Sea Process Study, U.S. JGOFS Planning Report No. 13. Woods Hole Oceanographic Institution, Woods Hole, Massachusetts, 164 pp.

Smith, S.L. (Ed.) 1998. 1994–1996 Arabian Sea Expedition: Oceanic Response to Monsoonal Forcing, Part 1. Deep-Sea Research 45, 1905–2501.

Smith, S.L. (Ed.) 1999. 1994–1996 Arabian Sea Expedition: Oceanic Response to Monsoonal Forcing, Part 2. Deep-Sea Research 46, 1531–1964

Smith, S.L. (Ed.) 2000. 1994–1996 Arabian Sea Expedition: Oceanic Response to Monsoonal Forcing, Part 3. Deep-Sea Research 47, 1177–1677.

Smith, S.L., 1984. Biological indications of active upwelling in the northeastern Indian Ocean and a comparison with Peru and northwest Africa. Deep-Sea Research 31, 951–967.

Smith, S.L., Codispoti, L.A., Morrison, J.M., Barber, R.T., 1998a. The 1994–1996 Arabian Sea Expedition: an integrated, interdisciplinary investigation of the response of the northwestern Indian Ocean to monsoonal forcing. Deep-Sea Research II 45, 1905–1915.

Smith, S.L., Roman, M., Prusova, I., Wishner, K., Gowing, M., Codispoti, L.A., Barber, R.T., Marra, J., Flagg, C.N., 1998b. Seasonal response of zooplankton to monsoonal reversals in the Arabian Sea. Deep-Sea Research II 45, 2369–2403.

Smith, W.O., Jr., R.T. Barber, M.R. Hiscock, J. Marra. The seasonal cycle of phytoplankton biomass and primary productivity in the Ross Sea, Antarctica. Deep-Sea Research, in press.

Stommel, H. M., 1965. The Gulf Stream. University of California Press, Berkeley, 248 pp.

Suess, E., 1980. Particulate organic carbon flux in the oceans: Surface productivity and oxygen utilization. Nature 288, 260–263.

Sverdrup, H.U., 1953. On conditions for the vernal blooming of phytoplankton. Journal du Conseil International pour Exploration de la Mer 18, 287–295.

Tindale, N.W., Pease, P.P., 1999. Aerosols over the Arabian Sea: Atmospheric transport pathways and concentrations of dust and sea salt. Deep-Sea Research II 46, 1577–1595.

Trees, C.C., Kenicutt, M.C., Brooks, J.M., 1985. Errors associated with the standard fluorometric determination of chlorophylls and phaeopigments. Marine Chemistry 17, 1–12.

Venrick, E.L., Hayward, T.L., 1984. Determining chlorophyll on the 1984 CalCOFI surveys. California Cooperative Oceanic Fisheries Investigation Report 25, 74–79.

Waite, A.M., Thompson, P.A., Harrison, P.J., 1992. Does energy control the sinking rates of marine diatoms? Limnology and Oceanography 37, 468–477.

Wassman, P., 1990. Relationships between primary and export production in the boreal coastal zone of the North Atlantic. Limnology and Oceanography 35, 464–471.

Weller, R.A., Baumgartner, M.F., Josey, S.A., Fischer, A.S., Kindle, J.C., 1998. Atmospheric forcing in the Arabian Sea during 1994–1995: observations and comparisons with climatology and models. Deep-Sea Research II 45, 1961–1999.

Welschmeyer, N.A., Strom, S., Goericke, R., DiTullio, G., Belvin, M., Peterson, W., 1993. Primary production in the subarctic Pacific Ocean: Project SUPER. Progress in Oceanography 32, 101–135.

Whitledge, T.E., Malloy, S.C., Patton, C.J., Wirick, C.D., 1981. Automated nutrient analyses in seawater. Brookhaven National Laboratory Report. BNL 51398, 216 pp.

Williams, P.J.leB., 1981. Microbial contributions to overall marine plankton metabolism: direct measurements of respiration. Oceanology Acta 4, 359–370.

Williams, P.J.leB., 1993a. Chemical and tracer methods of measuring plankton production. ICES Marine Science Symposia 197, 20–36.

Williams, P.J.leB., 1993b. On the definition of plankton production terms. ICES Marine Science Symposium 197, 9–19.

Williams, P.J.leB., 1995. Evidence for the seasonal accumulation of carbon-rich dissolved organic material, its scale in comparison with changes in particulate material and the consequential effect on net C/N assimilation ratios. Marine Chemistry 51, 17–29.

Williams, P.J.leB., Lefevre, D., 1996. Algal ^{14}C and total carbon metabolisms, 1 Models to account for the physiological processes of respiration and recycling. Journal of Plankton Research 18, 1941–1959.

Witter, A.E., Lewis, B.L., Luther, III, G.W., 2000. Iron speciation in the Arabian Sea. Deep-Sea Research II 47, 1517–1540.

Wüst, G., 1959. Proposed International Indian Ocean Expedition. Deep-Sea Research 6, 245–249.

Yoder, J.A., McClain, C.R., Geldman, G.C., Esaias, W.E., 1993. Annual cycles of phytoplankton chlorophyll concentrations in the global ocean: a satellite view. Global Biogeochemical Cycles 7, 181–193.

Young, D.K., Kindle, J.C., 1994. Physical processes affecting availability of dissolved silicate for diatom production in the Arabian Sea. Journal of Geophysical Research 99, 22619–22632.

Zeitzschel, B. (Ed.), 1973. The Biology of the Indian Ocean. Springer, New York, 549pp.